New *N*-phenylpyrrolamide DNA gyrase B inhibitors: Optimization of efficacy and antibacterial activity

Martina Durcik[a], **Denise Lovison**[a], **Žiga Skok**[a], **Cristina Durante Cruz**[b], **Päivi Tammela**[b], **Tihomir Tomaši** [a], **Davide Benedetto Tiz**[a], **Gábor Draskovits**[c], **Ákos Nyerges**[c], **Csaba Pál**[c], **Janez Ilaš**[a], **Lucija Peterlin Maši** [a], **Danijel Kikelj**[a], and **Nace Zidar**[a,*]

[a]Faculty of Pharmacy, University of Ljubljana, Ašker eva cesta 7, 1000, Ljubljana, Slovenia [b]Drug Research Program, Division of Pharmaceutical Biosciences, Faculty of Pharmacy, University of Helsinki, P.O. Box 56 (Viikinkaari 5 E), 00014, Helsinki, Finland [c]Synthetic and Systems Biology Unit, Institute of Biochemistry, Biological Research Centre of the Hungarian Academy of Sciences, Szeged, H-6726, Hungary

Abstract

The ATP binding site located on the subunit B of DNA gyrase is an attractive target for the development of new antibacterial agents. In recent decades, several small-molecule inhibitor classes have been discovered but none has so far reached the market. We present here the discovery of a promising new series of *N*-phenylpyrrolamides with low nanomolar IC_{50} values against DNA gyrase, and submicromolar IC_{50} values against topoisomerase IV from *Escherichia coli* and *Staphylococcus aureus.* The most potent compound in the series has an IC_{50} value of 13 nM against *E. coli* gyrase. Minimum inhibitory concentrations (MICs) against Gram-positive bacteria are in the low micromolar range. The oxadiazolone derivative **11a**, with an IC_{50} value of 85 nM against *E. coli* DNA gyrase displays the most potent antibacterial activity, with MIC values of 1.56 μM against *Enterococcus faecalis,* and 3.13 μM against wild type *S. aureus,* methicillin-resistant *S. aureus* (MRSA) and vancomycin-resistant *Enterococcus* (VRE). The activity against wild type *E. coli* in the presence of efflux pump inhibitor phenylalanine-arginine β-naphthylamide (PAβN) is 4.6 μM.

Keywords

Antibacterial; DNA gyrase; GyrB; Inhibitor; *N*-phenylpyrrolamide; ParE; Topoisomerase IV

* Corresponding author. nace.zidar@ffa.uni-lj.si (N. Zidar).

Author contributions
The manuscript was written using contributions from all authors. All authors have given approval to the final version of the manuscript.

Conflicts of interest
The authors declare no conflict of interest including any financial, personal or other relationships with other people or organizations.

1 Introduction

The discovery of antibacterials is considered to be one of the greatest medical achievements of all time. However, since the 1960s only a small number of new-class antibacterial agents have reached clinical practice while, on the other hand, the number of multi-drug resistant (MDR) bacteria is rising [1,2]. Nowadays, we are increasingly faced with life-threatening infections due to resistant Gram-positive and Gram-negative pathogens that belong to the "ESKAPE" group (*Enterococcus faecium, Staphylococcus aureus, Klebsiella pneumoniae, Acinetobacter baumannii, Pseudomonas aeruginosa,* and *Enterobacter* species). Thus, the ESKAPE pathogens were included by the World Health Organisation in the »WHO priority pathogens list for R&D of new antibiotics« [3,4].

DNA gyrase (gyrase) is a member of bacterial type IIA topoisomerase enzymes [5] that control the topology of DNA during processes of transcription, replication and recombination by introducing transient breaks to both DNA strands [6,7]. DNA gyrase helps relieve torsional tension by introducing negative supercoils to the DNA molecule during replication. It is a heterotetrameric protein composed of two GyrA subunits where the DNA cleavage site is located, and two GyrB subunits that provide the energy necessary for the catalytic function of the enzyme through ATP hydrolysis [6,8,9]. The four subunits form a functional tetramer A_2B_2. The other member of bacterial type IIA topoisomerases, topoisomerase IV (topo IV), is composed of two ParC and two ParE subunits that possess homologous structures to GyA and GyrB subunits of DNA gyrase. The main function of topo IV is decatenation of two daughter chromosomal DNA molecules after replication [8]. The structural and functional similarities of the two enzymes indicate that there is a possibility of designing inhibitors that target active sites of both gyrase and topo IV. This could reduce the capacity of bacteria to develop target-based drug resistance, since the probability of concurrent mutations on both targets is low [10]. Drugs targeting bacterial type IIA topoisomerases act by two main mechanisms, either by stabilizing the complex between a DNA molecule and the ParC/GyrA active site of the enzyme (e.g. quinolones), or by inhibiting the ATPase activity of the ParE/GyrB subunit (e.g. aminocoumarin class of inhibitors) [5,6]. Novobiocin, a representative of the natural aminocoumarins, is the only ATP-competitive inhibitor to have been used in the clinic but it has been withdrawn due to its toxicity and low effectiveness [11]. Studies of many co-crystal structures of ParE and GyrB subunits with small ligands and fragment-based design campaigns have led to several new classes of GyrB/ParE inhibitors being discovered (Fig. 1) [8,10]. However, none of them have advanced beyond phase I clinical trials, and most are only active against Gram-positive bacteria [10–12].

2 Results and discussion

2.1 Design

The design of the presented set of compounds was based on our previous *N*-phenylpyrrolamide inhibitors which had low nanomolar inhibitory activities against *E. coli* gyrase (IC_{50} < 100 nM). An example is compound D (Fig. 2a) [16]. The aim was to improve the GyrB/ParE binding affinity of compounds and their antibacterial activity by structural modifications, resulting in type I (Schemes 1–3) and type II (Scheme 4) compounds (Fig.

2b). For easier discussion, we have divided the structures into three parts: Part A, Part B and Part C (Fig. 2a).

To Part A, we introduced either a 4,5-dibromo-1*H*-pyrrole or a 3,4-dichloro-5-methyl-1*H*-pyrrole group. The pyrrole NH and pyrrolamide C=O groups are important hydrogen bond donor and acceptor groups that interact with Asp73 (*E. coli* numbering) and with a conserved water molecule (Fig. 2c) in the GyrB binding site. Halogen atoms on the pyrrole moiety lower the pK_a of the NH group and thus strengthen the formed H-bond. Chlorine and bromine atoms also increase the lipophilicity of the pyrrole moiety and thus increase hydrophobic interactions with the amino acid residues in the hydrophobic pocket of the enzyme (Val43, Ala47, Val71, Val167).

On the Part B benzene ring, compound D contains a lipophilic isopropoxy substituent that can form hydrophobic interactions with residues Ile78 and Ile94 in the lipophilic floor of the enzyme. Since these interactions were found to be favourable for the binding affinity, in some type I compounds (**7a-f, 8a-f, 10a, 11a** and **15a-b**) the isopropoxy group on the 3-position of the benzene ring was retained. To other type I compounds (**9a-e** and **12**) we introduced a 2-aminoethoxy substituent at this position, with the aim of improving the solubility of the compounds and/or broadening their antibacterial spectrum. Recently, the presence of an amino group, especially a primary amino group, was found to contribute to the ability of compounds to accumulate in Gram-negative *E. coli* [19]. With the type II compounds, we further explored the lipophilic floor of the enzyme by changing the position of substituents on the benzene ring from position 3- to 2-position. Similarly as in some type I compounds, in some type II compounds (**22c-d** and **23c-d**) we introduced the isopropoxy substituent to the 2-position of the benzene ring. In other type II compounds we introduced a sterically larger benzyloxy substituent (compounds **22a** and **23a**) or a basic 2-(dimethylamino)ethoxy substituent (compounds **22b** and **23b**), with the aim of enabling additional interactions with the enzyme and improving the water solubility of the compounds.

To Part C of type I compounds, groups that are able to form either ionic interactions with Arg136 side chain or π-stacking interactions with the Glu50-Arg76 salt bridge were attached. The influence of different α-amino acids attached to Part C was studied, aiming to determine how the stereochemistry and the size of the amino acid side chain affect the binding affinity. Thus, glycine, L- and D-alanine, L-valine, and L-phenylalanine derivatives were prepared. The activities of these derivatives, in the form of methyl esters, free carboxylic acids, and hydrazides, were compared. Additionally, three compounds (**11a, 11b** and **12**), each with a 1,3,4-oxadiazol-2-one ring as bioisosteric replacement for the carboxylic acid functionality, were prepared to reduce the acidity and polarity and thus improve bacterial cell membrane penetration of the compounds [20,21]. Furthermore, two compounds, each with a pyridine containing substituent in Part C, pyridin-2-ylmethanamine (n = 1, compound **15a**) and 2-(pyridin-2-yl) ethan-1-amine (n = 2, compound **15b**) were synthesized, and the optimal length for the activity determined. The pyridine moiety was intended to enable π-stacking interactions with the Glu50-Arg76 salt bridge.

2.2 Chemistry

The synthesis of type I compounds (**8a-i, 9a-e, 11a-b, 12, 15a-b**) is presented in Schemes 1–3. 3-Hydroxy-4-nitrobenzoic acid (**1**) was reacted with thionyl chloride in methanol to give methyl ester **2,** which was converted to **3a** in a Mitsunobu reaction using isopropanol, and to **3b** in the presence of potassium carbonate using *tert*-butyl (2-chloroethyl)carbamate as an alkylating agent. Compounds **3a-b** were hydrolysed with 1 M sodium hydroxide to give carboxylic acids **4a-b,** which were coupled with different amino acid methyl esters using TBTU (*N*,*N*,*N′*,*N′*-tetramethyl-*O*-(benzotriazol-1-yl)uronium tetrafluoroborate) in order to prepare amides **5a-g**. The nitro groups of **5a-g** were reduced by catalytic hydrogenation to give amines **6a-g.** Compounds **6a-g** were then coupled with 4,5-dibromopyrrole-2-carboxylic acid (to give **7a-c** and **7g-h**) or with 3,4-dichloro-5-methylpyrrole-2-carboxylic acid to give **7d-f** and **7i** in a two-step reaction. Oxalyl chloride was used to form pyrrole-2-carboxylic acid chloride in the first step followed by its aminolysis in pyridine in the second step. Products **8a-i** were prepared by alkaline hydrolysis of **7a-i.** Removal, by acidolysis, of the Boc protecting group from compounds **7h-i** and **8g-i** led to the final compounds **9a-e.** Compounds **7e** and **7i** were additionally reacted with hydrazine monohydrate under reflux to prepare hydrazides **10a-b.** These were converted to **11a-b** using 1,1′-carbonyldiimidazole (CDI) at 100 °C. The Boc protecting group was removed from **11b** to yield the target compound **12.**

To prepare products **15a-b, 4a** was first coupled with pyridin-2-ylmethanamine (to prepare **13a**) or 2-(pyridin-2-yl)ethan-1-amine (to prepare **13b**) using TBTU. Reducing the nitro groups of **13a-b** by catalytic hydrogenation led to compounds **14a-b.** The final products **15a-b** were prepared by coupling amines **14a-b** with 4,5-dibromopyrrole-2-carboxylic acid.

The synthesis of type II compounds (**23a-d**) is outlined in Scheme 4. 2-Hydroxy-4-nitrobenzoic acid (**16**) was converted to its methyl ester **17** using thionyl chloride in methanol. Compounds **18a-b** were prepared by reacting **17** with benzyl bromide or *β*-dimethyl-aminoethylchloride hydrochloride using potassium carbonate, while **18c** was synthesized under Mitsunobu conditions, using isopropyl alcohol. Alkaline hydrolysis of methyl esters **18a-c** led to carboxylic acids **19a-c,** which were coupled with glycine methyl ester hydrochloride, using TBTU, to give **20a-c.** The amines **21a-c** obtained after reduction of nitro groups of **20a-c** were coupled with either 4,5-dibromopyrrole-2-carboxylic acid to give **22a-c,** or 3,4-dichloro-5-methylpyrrole-2-carboxylic acid to give **22d.** Finally, methyl esters of **22a-d** were hydrolysed with 1 M sodium hydroxide to give target compounds **23a-d.**

2.3 Inhibitory activities against DNA gyrase and topoisomerase IV

All final compounds were evaluated for their inhibitory activity against *E. coli* DNA gyrase in a supercoiling assay. Results are presented as residual activities (RAs) of the enzyme at 1 μM of compounds or as IC_{50} values for compounds with RA < 50% (Tables 1 and 2). Compounds with submicromolar IC_{50} values were evaluated against *S. aureus* DNA gyrase, and *E. coli* and *S. aureus* topoisomerase IV (Table 3). To determine the possible binding modes of compounds, molecular docking of all tested compounds to the *E. coli* GyrB binding site was performed, using GOLD software [23].

Compounds **8e, 8f, 9b, 9e, 11a, 12, 23a** and **23d** showed inhibitory activities stronger than that of novobiocin (IC_{50} = 170 nM) against *E. coli* DNA gyrase, with low nanomolar inhibitory values (IC_{50} 91 nM). Seven of the eight most active compounds contained the 3,4-dichloro-5-methyl-1*H*-pyrrole moiety in Part A of the molecules, which thus proved to be more suitable than the 4,5-dibromo-1*H*-pyrrole moiety. The reason for this is probably the slightly smaller size of the chloro and methyl substituents than of the bromo substituents which bind to the hydrophobic pocket of the enzyme more strongly [16]. Compounds with free carboxylic acid groups in the eastern part of the molecules showed more potent activities than did their methyl ester analogues. For example, methyl ester **7f** was almost inactive at 1 μM concentration (RA = 87%), while its carboxylic acid derivative **8f** had an IC_{50} value of 41 nM and was among the most potent compounds of the series. Free carboxylic acids are able to form ionic interactions and/or hydrogen bonds with the Arg136 side chain in the binding site of the enzyme, while esters can only form hydrogen bonds, thus resulting in their weaker activity. A similar trend can be observed for other carboxylic acid – methyl ester pairs presented in Tables 1 and 2 The only methyl ester derivative with activity in the low nanomolar range was compound **9b,** with an IC_{50} value of 34 nM. Further, in some type I compounds (compounds **7e** and **7i),** methyl ester groups were converted to hydrazides (compounds **10a** and **10b),** which were then further converted to oxadiazolone rings (compounds **11a-b** and **12).** The activities of hydrazides (**10a,** IC_{50} = 280 nM) were weaker than those of the corresponding carboxylic acids (**8e,** IC_{50} = 38 nM) or oxadiazolones (**11a,** IC_{50} = 85 nM), probably because they cannot form ionic interactions with Arg136. On the other hand, both compound **8e** with a carboxylic acid group (IC_{50} = 38 nM) and its oxadiazolone containing analogue **11a** (IC_{50} = 85 nM) inhibited the enzyme in the low nanomolar range, although compound **8e** was approximately two-fold more potent. A different result was observed when oxadiazolone **12** (IC_{50} = 13 nM) was compared with its carboxylic acid analogue **9e** (IC_{50} = 28 nM), where the former was more potent. The only compound containing an oxadiazolone ring that did not show low nanomolar potency was **11b**, with an IC_{50} value of 1.6 μM, probably because it contains a side chain with the sterically larger *tert*-butyl carbamate group.

As reported recently [16], lipophilic substituents at the 3-position of the Part B benzene ring (e.g. methoxy, isopropoxy and benzyloxy substituents) form favourable interactions with the hydrophobic floor of the enzyme. In type I compounds, three different substituents have thus been introduced at this position: isopropoxy, 2-aminoethoxy and *N*-Boc-2-aminoethoxy substituents. Analogues with either an isopropoxy (**8e,** IC_{50} = 38 nM) or a 2-aminoethoxy substituent (**9e,** IC_{50} = 28 nM) had greater activity than analogues with an *N*-Boc-2-aminoethoxy substituent (**8i,** IC_{50} = 590 nM), probably because the *tert*-butyl carbamate group is too large to fit into the binding site of the enzyme. When compounds with isopropoxy and 2-aminoethoxy substituents were compared, the latter were generally more potent, as seen by comparing the isopropoxy derivatives **8d** (RA = 91% at 1 μM) and **7e** (RA = 66% at 1 μM) with their 2-aminoethoxy counterparts **9d** (IC_{50} = 370 nM) and **9b** (IC_{50} = 34 nM). Based on the docking experiments, it was predicted that the amino group of the 2-aminoethoxy substituent could form an H-bond with Ala100 that is part of the flexible loop formed by Gly97-Ser108 (compound **9e,** Fig. 3), thus increasing the inhibitory potency. Similarly, in the crystal structure of a bithiazole inhibitor in complex with *E. coli* GyrB

reported by Brvar et al. (PDB code: 4DUH [22]), a hydrogen bond was seen with Gly101 that is also a part of this loop. These interactions could stabilize the loop, reduce its flexibility and lead to stronger binding of the inhibitor.

To Part C of the type I compounds, we attached various amino acids: glycine, L- and D-alanine, L-valine and L-phenylalanine. Additionally, two compounds (**15a** and **15b**) were prepared with side chains containing a pyridine ring bound through either a methylene or an ethylene linker to the central benzamide core. Compounds with alanine side chains displayed the strongest inhibitory activity of the series while L-phenylalanine containing compounds were the weakest. For example, L-alanine analogue **8c** exhibited an IC_{50} value of 370 nM, while its L-phenylalanine containing counterpart **8b** was inactive at 1 μM concentration (RA = 100%). From these results it can be concluded that the benzyl group of the L-Phe side chain does not form favourable hydrophobic or π-π interactions with the enzyme. Furthermore, the size of the L-Phe group may force the molecule to take up an unfavourable conformation. Because of its size and flexibility, the benzyl group might be oriented out of the binding site towards the solvent, as was predicted with molecular docking of compound **8b** into the *E. coli* GyrB ATP-binding site (Fig. 1Sa, Supporting information). There were no marked differences in the activities of L-alanine (compound **8e,** $IC_{50} = 38$ nM) or D-alanine containing compounds (compound **8f,** $IC_{50} = 41$ nM). Compounds **15a** and **15b,** with pyridine containing groups, were not active against *E. coli* gyrase (RA = 100% or 87%). Even though the interaction between the pyridine nitrogen of compound **15a** and Arg76 was predicted by molecular docking, this side chain is probably too flexible to form a stable contact with Arg76 (Fig. 1Sb, Supporting information).

To further explore the binding site, type II compounds with substituents at the 2-position of the Part B benzene ring were prepared. Compounds with isopropoxy, benzyloxy and 2-dimethylaminoethoxy groups at this position were evaluated. As in type I compounds, only compounds with free carboxylic acid groups in the eastern part of the molecules showed nanomolar enzymatic inhibition. Compound **23b,** with a 2-dimethylaminoethoxy substituent (RA = 82% at 1 μM), showed the weakest activity of the series. The benzyloxy analogue **23a** ($IC_{50} = 88$ nM) was the most active type II compound, being 4-fold more active than its isopropoxy analogue **23c** ($IC_{50} = 400$ nM), indicating that it can form stronger hydrophobic interactions with the enzyme. A second very potent compound in the type II series was compound **23d** ($IC_{50} = 91$ nM) with an isopropoxy substituent on the benzene ring and a 3,4-dichloro-5-methylpyrrole group attached as Part A.

In general, the activities on DNA gyrase from *S. aureus* and on topo IV from *E. coli* and *S. aureus* were weaker than those on *E. coli* gyrase, but compounds **8e, 9e** and **12** that were among the most potent inhibitors of *E. coli* gyrase also displayed promising results on these three enzymes (Table 3). Compounds **8e, 9e** and **12** had IC_{50} values in the submicromolar range (<1 μM) against *E. coli* topo IV, which is much lower than that for novobiocin ($IC_{50} = 11$ μM). Compound **8e,** with an isopropoxy substituent, and compound **9e,** with aminoethoxy substituent on the 3-position of the benzene ring, additionally showed nanomolar IC_{50} values (93 nM and 110 nM, respectively) against *S. aureus* gyrase. Compound **8e** displayed the most balanced activities against all four tested enzymes, with a low IC_{50} of 280 nM also against *S. aureus* topo IV (IC_{50} of novobiocin is 27 μM) and thus

appears to be a promising dualtarget inhibitor. Interestingly, compound **8f**, a D-alanine analogue of **8e**, that showed an activity comparable to that of **8e** on DNA gyrase from *E. coli*, did not display the same potency on the other three enzymes. Since there are certain structural differences between the enzymes, the stereochemistry could be more important in the latter. A difference between **9e** and its methyl ester analogue **9b** was also observed, with weaker activities of the latter on all enzymes. These results correlate well with those for *E. coli* gyrase, leading to the assumption that an acidic functional group is also important for the binding to *S. aureus* gyrase and to topo IV from *E. coli* and *S. aureus.* Similarly, the carboxylic acid analogue **8e** displayed stronger activity than either the corresponding hydrazide **10a** or the oxadiazolone **11a** on these enzymes. Furthermore, the activity of the 3,4-dichloro-5-methyl-pyrrolamides (**8e, 8f, 8i, 9b, 9e, 10a, 11a, 12** and **23d**) was stronger than that of the 4,5-dibromopyrrolamides (**8c, 9d, 23a** and **23c**). The reason probably lies in the smaller size of the binding pockets of *S. aureus* DNA gyrase and of topo IV that results from differences in certain amino acid residues in the ATP binding site [25,26]. 3,4-Dichloro-5-methylpyrrolamides with smaller groups on the pyrrole ring bind more effectively to the enzyme.

2.4 Antibacterial activity

Compounds were tested for their antibacterial activity against two Gram-positive (*S. aureus* ATCC 25923 and *E. faecalis* ATCC 29212) and two Gram-negative (*E. coli* ATCC 25922 and *P. aeruginosa* ATCC 27853) wild type bacterial strains and, additionally, against two *E. coli* mutant strains (JW5503 *tolC* and JD17464 *lpxC*) at inhibitor concentrations of 50 μM. The *tolC* deletion mutant represents Gram-negative bacteria with defective efflux mechanisms and the *lpxC* deletion mutant represents a Gram-negative strain with disrupted bacterial cell wall. Results are presented in Table 1S (Supporting information) as percentages of growth inhibition. For compounds that inhibited bacterial strain growth by 80%, MIC values were also determined (Table 4).

Overall, the compounds displayed stronger inhibitory activity against Gram-positive than against Gram-negative bacteria. Nine compounds (**8a, 8d, 8e, 8f, 9a, 9b, 10a, 11a** and **11b**) showed more than 80% growth inhibition of *E. faecalis,* and three (**9a, 9b** and **11a**) inhibited the growth of *S. aureus* by more than 80%. Compound **9b,** with an aminoethoxy substituent on the 3-position of the central benzene ring, inhibited the growth of wild type *E. coli* by 67% (Table 1S) and completely suppressed the *E. coli tolC* deletion mutant at 50 μM. For compounds **7c, 8e, 8f, 9a, 11a** and **12,** significant differences in growth inhibition between wild type *E. coli* and the *E. coli* mutant strain having a defective efflux pump were also observed, while growth inhibition of the *E. coli* strain with impaired outer membrane was similar to that of the wild type for all compounds (Table 1S). These results suggest that some compounds are subject to bacterial efflux, which is probably the main reason for their weaker activity against Gram-negative bacteria.

Compound **11a** exhibited the strongest antibacterial activity of the series, with an MIC value of 1.56 μM against *E. faecalis,* which is almost two-fold lower than that of ciprofloxacin (3 μM), and of 3.13 μM against *S. aureus.* Compound **11a**, that contains an oxadiazolone ring in the eastern part of the molecule, was twice as active as its carboxylic acid analogue **8e** (*E.*

faecalis MIC = 3.13 μM) and four times more active than the corresponding hydrazide **10a** (*E. faecalis* MIC = 6.25 μM). This result is in agreement with our design strategy that compounds with a less acidic and less polar bioisostere for the carboxylic acid group could permeate bacterial membrane more easily and display stronger antibacterial activity. Compounds with an aminoethoxy substituent at the 3-position of the benzene ring (**9a, 9b** and **12**) exhibited no or weaker activity against *E. faecalis* (MIC values > 25 μM for **9a** and **9b** and no growth inhibition for compound **12**) than isopropoxy derivatives, presumably because the polarity of the amino group reduces the ability of compounds to enter the Gram-positive bacteria. Compounds containing both a free carboxylic acid group at the eastern part of the molecule and an aminoethoxy substituent at the 3-position of the benzene ring (**9c, 9d** and **9e**) were inactive against bacteria (less than 36% of growth inhibition, Table 1S) although compound **9e** was among the most active in enzyme assays (*S. aureus* gyrase IC$_{50}$ = 110 nM). On the other hand, compound **9b,** a methyl ester analogue of **9e** with a higher IC$_{50}$ value (*S. aureus* gyrase IC$_{50}$ = 390 nM), inhibited the growth of Gram-positive bacteria more strongly than **9e,** with MIC values of 50 μM against *S. aureus* and 25 μM against *E. faecalis* (Table 4). Additionally, compound **9b** showed a MIC value of 25 μM against an *E. coli* strain with defective efflux pump. Similar activities against an *E. coli* strain with a defective efflux pump were obtained for compound **9a** (MIC = 25 μM) and for compound **12** (MIC = 50 μM) that also contain an aminoethoxy substituent. These results suggest that the aminoethoxy substituent improves activity against Gram-negative bacteria, but the higher activity is not observed because the compounds are possible substrates for efflux pumps.

2.5   Advanced antibacterial evaluation of compound 11a

Compound **11a** was selected as the most promising of the series, since it had the low nanomolar IC$_{50}$ values in enzyme tests and the lowest MIC values against Gram-positive strains of all the compounds. For this reason, compound **11a** was further evaluated against a diverse panel of Gram-positive and Gram-negative bacterial strains (Table 5). In line with our previous observations, compound **11a** displayed an MIC value of 4.17 μM against the Gram-positive human pathogen *S. aureus* ATCC 29213. Furthermore, it was active against methicillin-resistant *Staphylococcus aureus* (MRSA, ATCC 43300) and vancomycin-resistant *Enterococcus* (VRE, ATCC 70022), with MICs of 3.13 μM (Table 5). On the other hand, compound **11a** displayed no bioactivity against wild type *E. coli* strains (ATCC 25922, MG1655 and BW 25113). We therefore sought to explore systematically the limiting factors for lack of anti-Gram-negative activity of compound **11a.** To investigate possible difficulties with its penetration into the bacterial cell, we tested compound **11a** on a diverse panel of mutant *E. coli* strains carrying loss-of-function mutations in either *dapF, mrcB* or *surA* genes that disrupt the bacterial cell wall integrity [27]. As a parallel approach, to test the susceptibility of compounds to efflux, we treated the parental strains and their corresponding mutants with an efflux pump inhibitor phenylalanine-arginine β-naphthylamide (PAβN), which is in fact not a typical inhibitor but a substrate for efflux pumps that is preferentially effluxed. Furthermore, we tested compound **11a** against *E. coli* BW 25113 Δ*acrB* and Δ*tolC* deletion mutants with defective efflux pumps. Mutations in the genes involved in the formation of the cell wall (*dapF, mrcB* and *surA*) did not increase the antibacterial activity (MIC > 50 μM) but, in the case of Δ*surA* strain, stronger inhibition was observed in the presence of PAβN (MIC = 13.8 μM). The presence of PAβN also increased the activity

against wild type *E. coli* strains ATCC 25922 (MIC = 4.6 μM) and MG1655 (MIC = 10.2 μM). Compound **11a** did not inhibit the efflux pump deficient *E. coli* BW 25113 strains Δ*acrB* and Δ*tolC* (MIC > 50 μM, Table 5), but it displayed weak activity against the *E. coli* JW5503 Δ*tolC* strain (51% inhibition at 50 μM, Table 1S). These results indicate that the most probable reason for the inactivity of compound **11a** against Gram-negative strains lies in bacterial efflux.

Additionally, in order to validate the interaction between the oxadiazolone ring of **11a** and Arg136 in the DNA gyrase binding site, compound **11a** was tested, in the presence of PAβN, on *E. coli* MG1655 strain with the Arg136 to Cys mutation. The compound was not active on the mutated bacteria (MIC > 50 μM), but displayed activity against wild type *E. coli* in the presence of PAβN (MIC = 10.2 μM), indicating that the compound interacts with Arg136.

2.6 Cytotoxic activity of compound 11a

The cytotoxicity of compound **11a** was determined by MTS assay against a human hepatocellular carcinoma cancer cell line (HepG2) and against human endothelial cells (HUVEC). The decrease in cell proliferation after the treatment with **11a** was compared with that after treatment with 50 μM of etoposide, as positive control. Compound **11a** showed no cytotoxicity against HepG2 cells at 50 μM (85% cell proliferation), while it showed an IC_{50} value of 40.7 μM against HUVEC cells (Table 2S, Supporting information). However, the concentration at which the compound was active against HUVEC cells was much higher than that at which it is active against Gram-positive bacteria.

3 Conclusions

Overall, thirty-eight compounds were designed, synthesized and evaluated against DNA gyrase and topoisomerase IV, and against several Gram-positive and Gram-negative bacterial strains. The most active compound in enzymatic assays was 3,4-dichloro-5-methyl-pyrrolamide **8e,** with an isopropoxy substituent at the 3-position of the benzene ring and a free carboxylic acid functionality in the eastern part of the molecule. Compound **8e** had an IC_{50} value of 38 nM against *E. coli* gyrase and 93 nM against *S. aureus* gyrase, and was also active against *E. coli* topo IV (IC_{50} = 0.45 μM) and *S. aureus* topo IV (IC_{50} = 0.28 μM). Compound **11a**, an oxadiazolone analogue of **8e,** possessed low micromolar antibacterial activity against Gram-positive bacteria, with MIC values of 1.56 μM and 3.13 μM against *E. faecalis* and *S. aureus,* respectively. Further, compound **11a** inhibited the growth of MRSA and VRE, key targets for antibiotic research, with MIC values of 3.13 μM [28]. Compound **11a** was not active against wild type *E. coli* strains, but was active in the presence of PAβN (MIC = 4.6 μM). These results suggest that, in Gram-negative bacteria, the compounds are sensitive to the efflux mechanism. In recent years, however, new compounds that can be used as adjuvants to potentiate the activity of antibiotics against Gram-negative strains are becoming available [29]. In short, low nanomolar enzymatic activity against DNA gyrase and topo IV, low micromolar MIC values against drug-resistant Gram-positive bacteria, and low cytotoxicity make compound **11a** a promising starting point for further optimization.

4 Experimental section

4.1 Determination of inhibitory activities on *E. coli* and *S. aureus* DNA gyrase

The assay for the determination of IC_{50} values was performed according to previously reported procedures [16].

4.2 Determination of inhibitory activities on *E. coli* and *S. aureus* topoisomerase IV

The assay for the determination of IC_{50} values was performed according to previously reported procedures [16].

4.3 Bacterial strains used in the study

Staphylococcus aureus ATCC 29213, *Staphylococcus aureus* ATCC 25923, *S. aureus* ATCC 43300, *Enterococcus faecalis* ATCC 29212, *Enterococcus faecium* ATCC 70022, *Escherichia coli* ATCC 25922, and *Pseudomonas aeruginosa* ATCC 27853 have been obtained from the American Type Culture Collection (ATCC) via Microbiologics Inc. (St. cloud, MN), *E. coli* MG1655 originated from the laboratory collection of Dr. Csaba Pál. *E. coli* BW 25113, and *E. coli* BW 25113 ΔacrB, ΔdapF, ΔmrcB and ΔsurA mutant strains originated from the KEIO collection [30]. Single-gene knock-out strains of *E. coli,* JW5503 ΔtolC [30] and JD17464 ΔlpxC were obtained from the NBRP-E.coli collection at the National Institute of Genetics (NIG, Japan).

4.4 Determination of antibacterial activity

The antibacterial activities against *S. aureus* ATCC 25923, *E. faecalis* ATCC 29212, *E. coli* ATCC 25922, *P. aeruginosa* ATCC 27853, *E. coli* JW5503, *E. coli* JD17464, S. *aureus* ATCC 43300, and *E. faecium* ATCC 70022 were determined following the CLSI guidelines and performed according to previously reported procedures [16].

MIC values against S. *aureus* ATCC 29213, *E. coli* ATCC 25922, *E. coli* MG1655, *E. coli* BW 25113, and *E. coli* BW 25113 ΔacrB, ΔdapF, ΔmrcB and ΔsurA were determined using a standard broth micro-dilution technique according to the EUCAST guidelines and ISO 20776-1:2006 [31]. In brief, 12-step serial dilutions of the test compound were prepared in 100 µL of cation adjusted Mueller-Hinton II Broth (Catalog n.o. 90922 from Merck KGaA, Darmstadt, Sigma) in 96-well microtiter plates. Approximately 5×10^4 bacteria were inoculated onto each well. Plates were incubated at 37 °C and shaken at 300 r.p.m. Measurements were performed in 3 replicates. After 18 h of incubation, optical density values were measured in a Biotek Synergy microplate reader at 600 nm wavelength for each well. MIC values were defined as the lowest concentration of the test substance where no visible growth can be observed, i.e. the background-normalized optical density of the culture at 600 nm was below 0.05.

4.5 *In vitro* cytotoxicity measurements

Cytotoxicity of compound **11a** was determined in MTS (3-(4,5-dimethylthiazol-2-yl)-5-(3-carboxymethoxyphenyl)-2-(4-sulfophenyl)-2*H*-tetrazolium) assay [32] with a few modifications. HepG2 (ATCC) and HUVEC (ATCC) cells were cultured in Eagle's MEM medium supplemented with L-glutamine (2 mM), penicillin/streptomycin (100 UI/mL/100

µg/mL), and 10% FBS. The cells were incubated in a humidified atmosphere with 5% CO_2 at 37 °C.

The cells were seeded in 96-well plates at densities 2000 cells per well in 100 µL of growth medium and incubated for 24 h to attach onto the wells. 50 µL of compounds at 50 µM in DMSO (0.5% final concentration) were added and incubated for 72 h. After 72 h 10 µL of CellTiter96® Aqueous One Solution Reagent, (Promega) [33] was added to determine the number of viable cells. The plates were incubated for another 3 h and absorbance (490 nm) was read with a BioTek's Synergy H4 microplate reader. Etoposide [IC_{50} = 20.1 µM (Ref. [34]: 30.2 µM) for HepG2 and IC_{50} = 5.21 µM (Ref. [35]: 1.25 µM) for HUVEC] at 50 µM was used as a positive control and 0.5% DMSO as a vehicle control. To determine cell viability, results from the wells that contained test compound-treated cells were compared to those with cells incubated in 0.5% DMSO. Independent experiments were run in triplicate and repeated two times. Statistical significance ($p < 0.05$) was calculated with two-tailed Welch's *t*-test between treated groups and DMSO. On HUVEC cell line, where compound showed higher activity, IC_{50} value (concentration of compound that inhibits cell proliferation by 50%) was determined using six concentrations of the tested compound. GraphPad Prism 5.0 software [36] was used to calculate the IC_{50} value.

4.6 Molecular modeling

4.6.1 Protein and ligand preparation—3D compound models were built using ChemBio3D Ultra 16.0 [37]. MMFF94 force field [38] was used for the optimization of geometries and partial atomic charges were added. Energy was minimized to less than 0.001 kcal/(mol Å) gradient value. The structure was refined with GAMESS interface using PM3 method, QA optimization algorithm and Gasteiger Hückel charges for all atoms for 100 steps [37]. GOLD Suite v5.4 [23,39] was used for molecular docking calculations. GOLD graphical user interface was used for receptor preparation. To the protein hydrogen atoms were added and correct tautomers and protonation states were assigned. Except for HOH614, all water molecules and ligands were deleted from the crystal structure. Amino acid residues within 7 Å around the ligand (PDB entry: 4DUH [22]) were selected as the binding site.

4.6.2 Ligand docking—Compounds were docked to the defined binding site in 25 independent genetic algorithm (GA) runs by applying different GA parameters (population size = 100, selection pressure = 1.1, number of operations = 100,000, niche size = 2, number of islands = 5, mutation frequency = 95, crossover frequency = 95, migration frequency = 10) and scoring functions (GoldScore, ChemScore, CHEMPLP). The most representative results were obtained using GoldScore as a scoring function. Ligands with RMSD value less than 1.5 Å were joined in clusters and early termination was allowed if the top 3 solutions were within 1.0 Å of the RMSD value. Proposed binding modes of the top 5 highest scored docking poses were evaluated for each ligand and the highest scored pose was used for graphical representation with PyMOL [24].

4.7   Chemistry

Chemicals were obtained from Acros Organics (Geel, Belgium), Sigma-Aldrich (St. Louis, MO, USA) and Apollo Scientific (Stockport, UK) and used without further purification. Analytical TLC was performed on silica gel Merck 60 F_{254} plates (0.25 mm), using visualization with UV light and spray reagents. Column chromatography was carried out on silica gel 60 (particle size 240–400 mesh). HPLC analyses were performed on an Agilent Technologies 1100 instrument (Agilent Technologies, Santa Clara, CA, USA) with a G1365B UV–Vis detector, a G1316A thermostat, a G1313A autosampler, and a ChemStation data system or on a Thermo Scientific Dionex Ultimate 3000 Binary Rapid Separation LC System (Thermo Fisher Scientific, Waltham, MA, USA) with an autosampler, a binary pump system, a photodiode array detector, a thermostated column compartment, and a Chromeleon Chromatography Data System. The eluent for consisted of trifluoroacetic acid (0.1% in water) or 20 mM phosphate buffer (pH 6.8) as solvent A and acetonitrile as solvent B. Two methods were used, method A: Agilent Eclipse Plus C18 column (5 μm, 4.6 mm × 150 mm), mobile phase of 30–90% of acetonitrile in TFA (0.1%) in 16 min, 90% acetonitrile to 20 min, a flow rate of 1.0 mL/min and a sample injection volume of 10 μL, and method B: Phenomenex Luna C18 column (5 μm, 4.6 mm × 250 mm), mobile phase of 50–80% of acetonitrile in 20 mM phosphate buffer (pH 6.8) in 30 min, a flow rate of 1.0 mL/min and a sample injection volume of 10 μL. Melting points were determined on a Reichert hot stage microscope and are uncorrected. ^{1}H and ^{13}C NMR spectra were recorded at 400 and 100 MHz, respectively, on a Bruker AVANCE III 400 spectrometer (Bruker Corporation, Billerica, MA, USA) in DMSO-d6, CDCl$_3$ or acetone–d_6 solutions, with TMS as the internal standard. IR spectra were recorded on a Thermo Nicolet Nexus 470 ESP FT-IR spectrometer (Thermo Fisher Scientific, Waltham, MA, USA). Mass spectra were obtained using a Q-TOF Premier mass spectrometer (Micromass, Waters, Manchester, UK) or ADVION expression CMSL mass spectrometer (Advion Inc., Ithaca, USA). Optical rotations were measured on a Perkin-Elmer 241 MC polarimeter. The reported values for specific rotation are average values of 10 successive measurements using an integration time of 5 s. The purity of the tested compounds was   95% as established by HPLC.

4.8   Synthetic procedures

4.8.1   General procedure A. Synthesis of Compounds 2 and 17 (with 2 as an Example)—To a suspension of 3-hydroxy-4-nitrobenzoic acid (**1**) (5.00 g, 27.3 mmol) in methanol (150 mL) cooled on ice bath thionyl chloride (5.90 mL, 81.9 mmol) was added dropwise. The mixture was stirred at rt for 15 h upon which a clear solution formed. The solvent was evaporated under reduced pressure. To the residue petroleum ether (50 mL) was added, the obtained suspension was sonicated, filtered and washed with petroleum ether (20 mL). The purification was repeated twice and the residue was dried to give compound **2** (4.92) as yellow crystals.

<u>**4.8.1.1   Methyl 3-hydroxy-4-nitrobenzoate (2) [40]:**</u> Yellow crystals; yield 92% (4.92 g); mp 87–88 °C (86–88 °C, lit [40]). IR (ATR) $v =$ 3309, 3053, 2961, 1720, 1623, 1586, 1434, 1321, 1220, 1146, 1097, 966, 842, 798, 743, 667 cm^{-1}. ^{1}H NMR (400 MHz, CDCl$_3$) δ 3.99 (s, 3H, CH$_3$), 7.64 (dd, 1H, $^3J =$ 8.8 Hz, $^4J =$ 1.6 Hz, Ar-H-6), 7.86 (d, 1H, $^4J =$ 1.6 Hz, Ar-H-2), 8.20 (d, 1H, $^3J =$ 8.8 Hz, Ar-H-5), 10.53 (s, 1H, OH).

4.8.2 General procedure B. Synthesis of Compounds 3a and 18c (with 3a as an Example)

—To a stirred solution of compound **2** (3.00 g, 15.2 mmol) and triphenylphosphine (5.40 g, 20.6 mmol) in anhydrous tetrahydrofuran (30 mL) isopropanol (1.5 mL, 19.8 mmol) was added and the mixture was stirred at rt for 10 min. Diisopropyl azodicarboxylate (DIAD, 3.90 mL, 19.8 mmol) was added dropwise and the mixture was stirred at rt for 15 h under argon atmosphere. The solvent was evaporated under reduced pressure and the crude product was purified with flash column chromatography using ethyl acetate/petroleum ether (1/6) as an eluent to give **3a** (3.50 g) as yellow solid.

4.8.2.1   Methyl 3-isopropoxy-4-nitrobenzoate (3a): Yellow solid; yield 97% (3.50 g); mp 42–44°C (39–41 °C, lit [41]). IR (ATR) $\nu = 3117, 2989, 2950, 1724, 1610, 1525, 1422, 1284, 1103, 1004, 942, 835, 741$ cm^{-1}. ^{1}H NMR (400 MHz, DMSO-d6) δ 1.30 (d, 6H, $^3J = 6.0$ Hz, CH(C<u>H</u>$_3$)$_2$), 3.91 (s, 3H, COOCH$_3$), 4.93 (spt, 1H, $^3J = 6.0$ Hz, C<u>H</u>(CH$_3$)$_2$), 7.64 (dd, 1H, $^3J = 8.4$ Hz, $^4J = 1.6$ Hz, Ar-H-6), 7.78 (d, 1H, $^4J = 1.2$ Hz, Ar-H-2), 7.95 (d, 1H, $^3J = 8.0$ Hz, Ar-H-5).

4.8.3 General procedure C. Synthesis of Compounds 4a-b and 19a-c (with 4a as an Example)

—To the solution of compound **3a** (3.50 g, 14.6 mmol) in methanol (30 mL) 1 M NaOH (28 mL, 29.3 mmol) was added. The mixture was stirred at rt for 15 h. The solvent was removed under reduced pressure and the residue acidified with 1 M HCl (10 mL). Water phase was extracted with ethyl acetate (3 × 20 mL). The combined organic phases were washed with water (3 × 20 mL) and brine (2 × 20 mL), dried over Na$_2$SO$_4$, filtered and the solvent removed under reduced pressure to afford **4a** (3.00 g) as yellow solid.

4.8.3.1   3-Isopropoxy-4-nitrobenzoic acid (4a): Yellow solid; yield 91% (3.00 g); mp 170–173 °C (173–175 °C, lit [41]). IR (ATR) $\nu = 1987, 2838, 2603, 1689, 1522, 1427, 1296, 110, 937, 837, 742$ cm^{-1}. ^{1}H NMR (400 MHz, DMSO-d6) δ 0.86 (d, 6H, $^3J = 6.0$ Hz, CH(C<u>H</u>$_3$)$_2$), 4.46 (spt, 1H, $^3J = 6.0$ Hz, C<u>H</u>(CH$_3$)$_2$), 7.17 (dd, 1H, $^3J = 8.0$ Hz, $^4J = 1.6$ Hz, Ar-H-6), 7.32 (d, 1H, $^4J = 1.6$ Hz, Ar-H-2), 7.48 (d, 1H, $^3J = 8.4$ Hz, Ar-H-5), 13.21 (s, 1H, COOH).

4.8.4 General procedure D. Synthesis of Compounds 5a-g, 13a-c and 20a-b (with 5a as an Example)

—To the suspension of **4a** (800 mg, 3.55 mmol) and TBTU (1.48 g, 4.62 mmol) in dichloromethane (40 mL) *N*-methylmorpholine (1.2 mL, 10.7 mmol) was added. The reaction mixture was stirred at rt for 30 min upon which a clear solution formed. L-valine methyl ester hydrochloride (715 mg, 4.26 mmol) was added and the mixture was stirred at rt for 15 h. The solvent was removed under reduced pressure and the residue was dissolved in ethyl acetate (30 mL) and water (30 mL). The organic phase was washed with saturated aqueous NaHCO$_3$ solution (3 × 20 mL) and brine (2 × 20 mL), dried over Na$_2$SO$_4$, filtered and the solvent evaporated under reduced pressure to give **5a** (1.11 g) as yellow oil.

4.8.4.1   Methyl (3-isopropoxy-4-nitrobenzoyl)-L-valinate (5a): Yellow oil; yield 92% (1.11 g); $[\alpha]_D^{25}$ -8.32 (c 0.263, MeOH). IR (ATR) $\nu = 3279, 2974, 1744, 1640, 1533, 1317,$

1256, 1103, 1021, 842, 748 cm^{-1}. ^{1}H NMR (400 MHz, CDCl$_3$) δ 1.00–1.04 (m, 6H, CHCH(C$\underline{H}_3$)$_2$), 1.42 (d, 6H, ^3J = 6 Hz, OCH(C$\underline{H}_3$)$_2$), 2.27–2.35 (m, 1H, C$\underline{H}$CH(CH$_3$)$_2$), 3.81 (s, 3H, COOC$\underline{H}_3$), 4.75–4.82 (m, 2H, CHC$\underline{H}$(CH$_3$)$_2$, OC$\underline{H}$(CH$_3$)$_2$), 6.71 (d, 1H, ^3J = 8.4 Hz, NH), 7.31 (dd, 1H, ^3J = 8.4 Hz, ^4J = 1.6 Hz, Ar-H-6), 7.62 (d, 1H, ^4J = 1.2 Hz, Ar-H-2), 7.81 (d, 1H, ^3J = 8.0 Hz, Ar-H-5). ^{13}C NMR (100 MHz, DMSO-d6) δ 19.01 (CH$_3$), 19.10 (CH$_3$), 21.50 (CH($\underline{C}$H$_3$)$_2$), 21.56 (CH($\underline{C}$H$_3$)$_2$), 29.60 (CH), 51.75 (COO$\underline{C}$H$_3$), 58.77 (CH), 72.43 (CH), 115.32, 119.76, 124.62, 138.42, 142.29, 149.61, 165.28 (CONH), 171.97 ($\underline{C}$OOCH$_3$).

4.8.5 General procedure E. Synthesis of Compounds 6a-g, 14b-c and 21a-b (with 6a as an Example)

—Compound **5a** (1.11 g, 3.28 mmol) was dissolved in methanol (40 mL), Pd/C (111 mg) was added and the reaction mixture was stirred under hydrogen atmosphere for 3 h. The catalyst was filtered off and the solvent removed under reduced pressure.

4.8.5.1   Methyl (4-amino-3-isopropoxybenzoyl)-L-valinate (6a): The crude product was purified with flash column chromatography using ethyl acetate/petroleum ether (1/1) as an eluent to obtain **6a** (522 mg) as yellow oil. Yield: 55% (522 mg). [α]$_D^{25}$ -5.53 (c 0.378, MeOH). ^{1}H NMR (400 MHz, CDCl$_3$) δ 0.99–1.03 (m, 6H, CHCH(C$\underline{H}_3$)$_2$), 1.38 (d, 6H, ^3J = 6.4 Hz, OCH(C$\underline{H}_3$)$_2$), 2.23–2.31 (m, 1H, CHC$\underline{H}$(CH$_3$)$_2$), 3.79 (s, 1H, COOC$\underline{H}_3$), 4.11–4.17 (m, 2H NH$_2$), 4.66 (spt, 1H, ^3J = 6.0 Hz, OC$\underline{H}$(CH$_3$)$_2$), 4.76–4.79 (m, 1H, C$\underline{H}$CH(CH$_3$)$_2$), 6.50 (d, 1H, ^3J = 8.8 Hz, NH), 6.70 (d, 1H, ^3J = 8.0 Hz, Ar-H-5), 7.20 (dd, 1H, ^3J = 8.0 Hz, ^4J = 2.0 Hz, Ar-H-6), 7.40 (d, 1H, ^4J = 2.0 Hz, Ar-H-2). MS (ESI) m/z = 331.37 ([M+Na]$^+$).

4.8.6 General procedure F. Synthesis of Compounds 7a-i, 15a-d and 22a-b (with 7a as an Example)

—To a solution of 4,5-dibromo-1H-pyrrole-2-carboxylic acid (157 mg, 0.584 mmol) in anhydrous dichloromethane (4 mL) oxalyl chloride (2 M solution in dichloromethane, 1.46 mL, 2.92 mmol) was added dropwise and the solution stirred at rt for 15 h under argon atmosphere. The solvent was evaporated under reduced pressure, fresh anhydrous dichloromethane (4 mL), **6a** (150 mg, 0.487 mmol) and pyridine (2 mL) were added and the reaction mixture stirred under argon atmosphere at rt for 15 h. Solvent was removed under reduced pressure, the residue dissolved in ethyl acetate (20 mL) and washed with water (20 mL), saturated aqueous NaHCO$_3$ solution (3 × 20 mL) and brine (2 × 20 mL). The organic phase was dried over Na$_2$SO$_4$, filtered and the solvent removed under reduced pressure.

4.8.6.1   Methyl (4-(4,5-dibromo-1H-pyrrole-2-carboxamido)-3-isopropoxybenzoyl)-L-valinate (7a): To the crude product ethyl acetate and petroleum ether (1:2, 15 mL) were added and the precipitate was filtered off to obtain **7a** (40 mg) as light brown solid. The mother liquid was concentrated and purified with flash column chromatography using ethyl acetate/petroleum ether (1/2) as an eluent to give another 61 mg of **7a** as light brown solid. Yield 37% (101 mg); mp 145–148 °C [α]$_D^{25}$ +8.94 (c 0.273, MeOH). IR (ATR) ν = 3417, 3304, 3238, 2964, 1741, 1633, 1515, 1418, 1311, 1202, 1124, 978, 831, 743 cm^{-1}. ^{1}H NMR (400 MHz, DMSO-d6) δ 0.94–1.00 (m, 6H, CHCH(C$\underline{H}_3$)$_2$), 1.32–1.35 (m, 6H, OCH(C$\underline{H}_3$)$_2$), 2.15–2.23 (m, 1H, CHC$\underline{H}$(CH$_3$)$_2$), 3.67 (s, 3H, COOC$\underline{H}_3$), 4.30 (t, 1H, ^3J =

8.0 Hz, CHCH(CH$_3$)$_2$), 4.72 (spt, 1H, ^3J = 6.0 Hz, OCH(CH$_3$)$_2$), 7.18 (d, 1H, ^4J = 2.4 Hz, Pyrr-CH), 7.53–7.55 (m, 2H, Ar-H-2,6), 7.92 (d, 1H, ^3J = 8.4 Hz, Ar-H-5), 8.59 (d, 1H, ^3J = 8.0 Hz, CONHCH), 9.06 (s, 1H, CONHAr), 13.02 (d, 1H, ^4J = 2.8 Hz, Pyrr-NH). ^{13}C NMR (100 MHz, DMSO-d6) δ 19.06 (CHCH(CH$_3$)$_2$), 19.09 (CHCH(CH$_3$)$_2$), 21.59 (OCH(CH$_3$)$_2$), 21.67 (OCH(CH$_3$)$_2$), 29.45 (CHCH(CH$_3$)$_2$), 51.55 (COOCH$_3$), 58.59 (CHCH(CH$_3$)$_2$), 71.29 (OCH(CH$_3$)$_2$), 98.35, 106.22, 113.18, 113.77, 120.11, 122.44, 127.50, 130.06, 130.50, 148.15, 156.95, 166.15 (Ar-CONH), 172.26 (COOCH$_3$). MS (ESI) m/z = 556.0 ([M-H]$^-$), HRMS for C$_{21}$H$_{24}$Br$_2$N$_3$O$_5$: calculated 556.0083, found 556.0076. HPLC: t_r 14.108 min (97.2% at 280 nm, method A).

4.8.7 General procedure G. Synthesis of Compounds 8a-e, 8g-i and 23a-d (with 8a as an Example)

To the solution of **7a** (65 mg, 0.116 mmol) in tetrahydrofuran (8 mL) 1 M NaOH (348 µL, 348 µmol) was added and the mixture was stirred at rt for 15 h. The solvent was evaporated under reduced pressure, the residue acidified with 1 M HCl (5 mL) to pH 1 and the water phase was extracted with ethyl acetate (3 × 10 mL). The combined organic phases were washed with water (3 × 10 mL) and brine (10 mL), dried over Na$_2$SO$_4$, filtered and the solvent removed under reduced pressure to obtain **8a** (53 mg) as white solid.

4.8.7.1 (4-(4,5-Dibromo-1H-pyrrole-2-carboxamido)-3-isopropoxybenzoyl)-L-valine (8a):

White solid; **y**ield 87% (53 mg); mp 116–120 °C; [α]$_D^{25}$ +18.6 (c 0.288, MeOH). IR (ATR) ν = 3402, 3183, 2970, 1716, 1648, 1507, 1389, 1265, 1179, 1109, 977, 805, 751 cm^{-1}. ^{1}H NMR (400 MHz, DMSO-d6) δ 0.96–1.00 (m, 6H, CHCH(CH$_3$)$_2$), 1.32–1.36 (m, 6H, OCH(CH$_3$)$_2$), 2.15–2.22 (m, 1H, CHCH(CH$_3$)$_2$), 4.30 (t, 1H, ^3J = 8.0 Hz, CHCH(CH$_3$)$_2$), 4.73 (spt, 1H, ^3J = 5.6 Hz, OCH(CH$_3$)$_2$), 7.18 (d, 1H, ^4J = 2.4 Hz, Pyrr-CH), 7.53–7.57 (m, 2H, Ar-H-2,6), 7.92 (d, 1H, ^3J = 8.0 Hz, Ar-H-5), 8.42 (d, 1H, ^3J = 8.0 Hz, CONHCH), 9.05 (s, 1H, CONHAr), 12.62 (br s, 1H, COOH), 13.02 (s, 1H, Pyrr-NH). ^{13}C NMR (100 MHz, DMSO-d6) δ 18.89 (CHCH(CH$_3$)$_2$), 19.34 (CHCH(CH$_3$)$_2$), 21.67 (OCH(CH$_3$)$_2$), 21.76 (OCH(CH$_3$)$_2$), 29.52 (CHCH(CH$_3$)$_2$), 58.38 (CHCH(CH$_3$)$_2$), 71.36 (OCH(CH$_3$)$_2$), 98.41, 106.28, 113.28, 113.82, 120.16, 122.53, 127.60, 130.43, 130.46, 148.22, 157.03, 166.13 (Ar-CONH), 173.22 (COOH). MS (ESI) m/z = 542.0 ([M-H]$^-$), HRMS for C$_{20}$H$_{22}$Br$_2$N$_3$O$_5$: calculated 541.9926, found 541.9935. HPLC: t_r 12.049 min (98.1% at 280 nm, method A).

4.8.8 General procedure H. Synthesis of Compounds 9a-e (with 9a as an Example)

The starting compound (**7h,** 40 mg, 0.057 mmol) was dissolved in 4M HCl in 1,4-dioxane (4 mL) and tetrahydrofuran (1 mL) and the reaction mixture stirred at rt for 2 h. The solvent was removed under reduced pressure, to the residue diethyl ether (10 mL) was added, the obtained suspension was sonicated, filtered, washed with diethyl ether (2 × 2 mL) and dried to give **9a** (36 mg) as white solid.

4.8.8.1 (S)-2-(2-(4,5-Dibromo-1H-pyrrole-2-carboxamido)-5-((1-methoxy-1-oxo-3-phenylpropan-2-yl)carbamoyl)phenoxy)ethan-1-aminium chloride (9a):

White solid; **y**ield 99% (36 mg); mp 146–148 °C; [α]$_D^{25}$ -48.7 (c 0.252, MeOH). IR (ATR) ν = 3394, 3326, 3222, 3029, 2951, 2859, 1723, 1649, 1509, 1414, 1277, 1179, 1021, 972, 816, 746, 700 cm^{-1}. ^{1}H NMR (400 MHz, DMSO-d6) δ 3.09–3.21 (m, 2H, CH$_2$Ph), 3.38–3.43 (m, 2H,

OCH$_2$CH$_2$NH, overlapping with the signal for water), 3.65 (s, 3H, CH$_3$), 4.30 (t, 2H, ^3J = 4.4 Hz, OCH$_2$CH$_2$NH), 4.64–4.70 (m, 1H, CH), 7.18–7.36 (m, 6H, 5 × Ar-H, Pyrr-CH), 7.48 (d, 1H, ^4J = 1.6 Hz, Ar-H), 7.51 (dd, 1H, ^3J = 8.4 Hz, ^4J = 1.6 Hz, Ar-H), 8.03 (d, 1H, ^3J = 8.4 Hz, Ar-H), 8.25 (s, 3H, NH$_3^+$), 8.89 (d, 1H, ^3J = 8.0 Hz, CONHCH), 9.44 (s, 1H, CONHAr), 13.10 (d, 1H, ^4J = 2.4 Hz, Pyrr-NH). ^{13}C NMR (100 MHz, DMSO-d6) δ 36.25 (CH$_2$), 38.35 (CH$_2$), 51.95 (CH$_3$), 54.33 (CH), 64.84 (CH$_2$), 98.41, 106.29, 110.57, 115.03, 120.24, 122.13, 126.49, 127.47, 128.24, 129.07, 129.51, 129.53, 137.66, 147.98, 157.29, 165.54 (Ar-CONH), 172.21 (COOH). MS (ESI) m/z = 605.0 ([M-H]$^-$). HRMS for C$_{24}$H$_{23}$Br$_2$N$_4$O$_5$: calculated 605.0035, found 605.0018. HPLC: t_r 8.015 min (95.0% at 220 nm, 95.3% at 280 nm, method A).

4.8.9 General procedure I. Synthesis of Compounds 10a-b (with 10a as an Example)—To the solution of **7e** (180 mg, 0.395 mmol) in anhydrous methanol and anhydrous tetrahydrofurane (3:1, 16 mL) hydrazine monohydrate (240 μL, 3.95 mmol) was added and the reaction mixture stirred at 65 °C for 15 h. The obtained suspension was cooled on ice bath, the precipitate filtered off and dried to give **10a** (104 mg) as white solid.

4.8.9.1   (S)-3,4-Dichloro-N-(4-((1-hydrazineyl-1-oxopropan-2-yl) carbamoyl)-2-isopropoxyphenyl)-5-methyl-1H-pyrrole-2-carboxamide (10a): White solid; yield 58% (104 mg); mp 235–237 °C [α]$_D^{25}$ +87.9 (c 0.220, DMF). IR (ATR) ν = 3397, 3365, 3310, 3252, 3134, 2984, 2940, 1733, 1648, 1518, 1441, 1324, 1261, 1173, 1042, 990, 831, 747, 702 cm^{-1}. ^{1}H NMR (400 MHz, DMSO-d6) δ 1.32–1.38 (m, 9H, CH$_3$, CH(CH$_3$)$_2$), 2.24 (s, 3H, Pyrr-CH$_3$), 4.23 (s, 2H, NH$_2$), 4.47 (quint, 1H, ^3J = 7.2 Hz, CONHCH), 4.88 (spt, 1H, ^3J = 6.0 Hz, CH(CH$_3$)$_2$), 7.56 (dd, 1H, ^3J = 8.4 Hz, ^4J = 1.6 Hz, Ar-H-6), 7.64 (d, 1H, ^4J = 1.6 Hz, Ar-H-2), 8.44–8.48 (m, 2H, Ar-H-5, CONHCH), 9.18 (s, 1H, NHNH$_2$), 9.25 (s, 1H, CONHAr), 12.45 (s, 1H, Pyrr-NH); ^{13}C NMR (100 MHz, DMSO-d6) δ 10.75 (Pyrr-CH$_3$), 18.16 (CH$_3$), 21.78 (CH(CH$_3$)$_2$), 21.84 (CH(CH$_3$)$_2$), 47.67 (CH), 71.28 (CH(CH$_3$)$_2$), 108.58, 109.67, 111.89, 117.87, 118.66, 120.65, 128.92, 129.75, 131.01, 145.05, 156.19, 165.22 (Ar-CONH), 171.77 (CONHNH$_2$). MS (ESI) m/z = 454.1 ([M-H]$^-$). HRMS for C$_{19}$H$_{22}$Cl$_2$N$_5$O$_4$: calculated 454.1049, found 454.1041. HPLC: t_r 9.111 min (95.8% at 254 nm, method A).

4.8.10   General procedure J. Synthesis of Compounds 11a-b (with 11a as an Example)—To the solution of **10a** (83 mg, 0.172 mmol) in 1,4-dioxane and anhydrous dimethylformamide (2:1, 7.5 mL) 1,1′-carbonyldiimidazole (CDI, 55.8 mg, 0.344 mmol) was added and the reaction mixture was stirred at 101 °C for 15 h. Additional 0.5 equivalents of 1,1′-carbonyldiimidazole (14 mg, 0.0863 mmol) were added and the mixture was stirred at 101 °C for 1 h. The solvent was removed under reduced pressure.

4.8.10.1   (S)-3,4-Dichloro-N-(2-isopropoxy-4-((1-(5-oxo-4,5-dihydro-1,3,4-oxadiazol-2-yl)ethyl)carbamoyl)phenyl)-5-methyl-1H-pyrrole-2-carboxamide (11a): To the residue acetonitrile (10 mL) was added, the obtained suspension was sonicated and filtered. To the precipitate water (10 mL) was added, the suspension was sonciated, filtered, washed with water (2 × 5 mL) and dried to obtain **11a** (48 mg) as an off-white solid. Yield 58% (48 mg);

mp 244–246°C; $[\alpha]_D^{25}$ +37.9 (c 0.463, DMF). IR (ATR) ν = 3397, 3361, 3232, 3136, 2981, 2923, 2852, 1775, 1649, 1514, 1415, 1322, 1260, 1175, 1110, 917, 831, 759, 702 cm^{-1}. ^{1}H NMR (400 MHz, DMSO-d6) δ 1.36–1.37 (m, 6H, CH(C$\underline{H}_3)_2$), 1.49 (d, 3H, ^3J = 6.8 Hz, CH$_3$), 2.24 (s, 3H, Pyrr-CH$_3$), 4.86 (spt, 1H, ^3J = 6.0 Hz, C$\underline{H}$(CH$_3)_2$), 5.11 (quint, 1H, ^3J = 7.2 Hz, Hz, CONHC$\underline{H}$), 7.55–7.61 (m, 2H, 2 × Ar-H), 8.47 (d, 1H, ^3J = 8.4 Hz, Ar-H-5), 8.88 (d, 1H, ^3J = 7.6 Hz, CON$\underline{H}$CH), 9.26 (s, 1H, CONHAr), 12.27 (br s, 1H, oxadiazolone-NH/Pyrr-NH), 12.45 (s, 1H, oxadiazolone-NH/Pyrr-NH). ^{13}C NMR (100 MHz, DMSO-d6) δ 10.76 (Pyrr-CH$_3$), 16.87 (CH$_3$), 21.77 (CH($\underline{C}$H$_3)_2$), 21.80 (CH($\underline{C}$H$_3)_2$), 41.73 (CH), 71.36 ($\underline{C}$H(CH$_3)_2$), 108.60, 109.74, 111.65, 117.99, 118.63, 120.55, 128.28, 129.82, 131.35, 145.20, 154.89, 156.22, 157.23, 165.10 (Ar-$\underline{C}$ONH). MS (ESI) m/z = 480.1 ([M-H]$^-$). HRMS for C$_{20}$H$_{20}$Cl$_2$N$_5$O$_5$: calculated 480.0841, found 480.0848. HPLC: t_r 12.275 min (95.2% at 220 nm, method A).

4.8.10.2   (S)-2-(2-(3,4-Dichloro-5-methyl-1H-pyrrole-2-carboxamido)-5-((1-(5-oxo-4,5-dihydro-1,3,4-oxadiazol-2-yl)ethyl) carbamoyl)phenoxy)ethan-1-aminium chloride (12):
Synthesized according to General procedure H with stirring the reaction mixture for 5 h. The product was additionally purified with reverse-phase flash chromatography on a Biotage Isolera One System using a Biotage SNAP Cartridge KP-C18-HS 12 g column and 15–60% acetonitrile in TFA (0.1%) as a mobile phase to afford **12** (5 mg) as an off white solid. Yield 16% (5 mg); mp 234–236 °C; $[\alpha]_D^{25}$ +29.6 (c 0.180, MeOH). ^{1}H NMR (400 MHz, DMSO-d6) δ 1.50 (d, 3H, ^3J = 7.6 Hz, CH$_3$), 2.25 (s, 3H, Pyrr-CH$_3$), 3.34 (2H, OCH$_2$C$\underline{H}_2$NH$_3^+$, overlapping with the signal for water), 4.39 (t, 2H, ^3J = 4.4 Hz, OC$\underline{H}_2$CH$_2$NH$_3^+$), 5.11 (quint, 1H, ^3J = 7.2 Hz, CONHC$\underline{H}$), 7.61–7.62 (m, 2H, Ar-H-4,6), 8.24 (s, 3H, NH$_3^+$), 8.41 (d, 1H, ^3J = 8.8 Hz, Ar-H-3), 8.98 (d, 1H, ^3J = 7.6 Hz, CON$\underline{H}$CH), 9.26 (s, 1H, CONHAr), 12.31 (s, 1H, oxadiazole-NH/Pyrr-NH), 12.51 (s, 1H, oxadiazole-NH/Pyrr-NH). MS (ESI) m/z = 484.1 ([M-H]$^+$). HRMS for C$_{19}$H$_{20}$Cl$_2$N$_5$O$_6$: calculated 484.0791, found 484.0798. HPLC: t_r 3.697 (97.8% pri 280 nm, method A).

4.8.10.3   3-Isopropoxy-4-nitro-N-(pyridin-2-ylmethyl)benzamide (13a):
Synthesized according to General procedure D with pyridin-2-ylmethanamine (420 μL, 3.73 mmol) as a reagent. The crude product was purified with flash column chromatography using dichloromethane/methanol (20/1) as an eluent to give **13a** (612 mg) as pale yellow solid. Yield 66% (612 mg); mp 73–75 °C. IR (ATR) ν = 3192, 2991, 2937, 1656, 1517, 1412, 1357, 1301, 1253, 1103, 1008, 960, 837, 751 cm^{-1}. ^{1}H NMR (400 MHz, CDCl$_3$) δ 1.44 (d, 6H, ^3J = 6.4 Hz, CH(C$\underline{H}_3)_2$), 4.78 (d, 2H, ^3J = 4.4 Hz, CH$_2$), 4.82 (spt, 1H, ^3J = 6.4 Hz, C$\underline{H}$(CH$_3)_2$), 7.26–7.27 (m, 1H, NH/Ar-H-2), 7.29–7.30 (m, 1H, NH/Ar-H-2), 7.35 (d, 1H, ^3J = 8.0 Hz, Ar-H-5), 7.40 (dd, 1H, ^3J = 8.4 Hz, ^4J = 1.6 Hz, Ar-H-6), 7.70–7.84 (m, 4H, 4 × Pyridine-H), 8.59–8.61 (d, 1H, NH). ^{13}C NMR (100 MHz, DMSO-d6) δ 21.58 (CH($\underline{C}$H$_3)_2$), 44.86 (CH$_2$), 72.38 ($\underline{C}$H(CH$_3)_2$), 114.91, 119.40, 121.12, 122.21, 124.76, 136.78, 138.76, 142.15, 148.91, 149.76, 158.28, 164.60 (CONH). MS (ESI) m/z = 314.38 ([M-H]$^-$).

4.8.10.4   4-Amino-3-isopropoxy-N-(pyridin-2-ylmethyl)benzamide (14a):
Synthesized according to General procedure E with stirring the reaction mixture for 4 h. Yellow oil; yield

99% (230 mg). IR (ATR) ν = 3464, 3289, 3170, 2978, 1622, 1546, 1506, 1303, 1225, 1110, 956, 825, 754, 608 cm^{-1}. ^{1}H NMR (400 MHz, DMSO-d6) δ 1.29 (d, 6H, ^3J = 6.0 Hz, CH(C$\underline{H}_3$)$_2$), 4.52 (d, 2H, ^3J = 6 Hz, CH$_2$), 4.56 (spt, 1H, ^3J = 6 Hz, C$\underline{H}$(CH$_3$)$_2$), 5.22 (s, 2H, NH$_2$), 6.64 (d, 1H, ^3J = 8.0 Hz, Ar-H-5), 7.24–7.29 (m, 2H, 2 × Pyridine-H), 7.35 (dd, 1H, ^3J = 8.0Hz, ^4J = 2.0 Hz, Ar-H-6), 7.40 (d, 1H, ^4J = 2.0 Hz, Ar-H-2), 7.73–7.77 (td, 1H, Pyridine-H), 8.49–8.51 (dq, 1H, Pyridine-H), 8.72 (t, 1H, ^3J = 6.0 Hz, NH). ^{13}C NMR (100 MHz, DMSO-d6) δ 21.96 (CH($\underline{C}H_3$)$_2$), 44.57 (CH$_2$), 70.28 ($\underline{C}H$(CH$_3$)$_2$), 112.55, 112.91, 120.83, 121.24, 121.33, 121.91, 136.61, 142.39, 143.09, 148.70, 159.43, 166.27 (CONH). MS (ESI) m/z = 284.39 ([M-H]$^-$).

4.8.10.5 4,5-Dibromo-N-(2-isopropoxy-4-((pyridin-2-ylmethyl)carbamoyl)phenyl)-1H-pyrrole-2-carboxamide (15a): Synthesized according to General procedure F but a few seconds after the addition of pyridine a precipitate started to form which was filtered off and washed with methanol (10 mL) to give **15a** (37 mg) as white solid. Yield 13% (37 mg); mp 253–255 °C. IR (ATR) ν = 3383, 2976, 2633, 1652, 1521, 1402, 1310, 1274, 1201, 1127, 967, 874, 753 cm^{-1}. ^{1}H NMR (400 MHz, DMSO-d6) δ 1.34 (d, 6H, ^3J = 6.0 Hz, CH(C$\underline{H}_3$)$_2$), 4.62 (d, 2H, ^3J = 5.6 Hz, CH$_2$), 4.71 (spt, 1H, ^3J = 6.0 Hz, C$\underline{H}$(CH$_3$)$_2$), 7.18 (d, 1H, ^4J = 2.4 Hz, Pyrr-CH), 7.36–7.39 (m, 1H, Pyridine-H), 7.43 (d, 1H, ^3J = 7.6 Hz, Pyridine-H), 7.56 (dd, 1H, ^3J = 8.0 Hz, ^4J = 1.6 Hz, Ar-H-6), 7.62 (d, 1H, ^4J = 1.6 Hz, Ar-H-2), 7.86–7.90 (td, 1H, Pyridine-H), 7.94 (d, 1H, ^3J = 8.0 Hz, Ar-H-5), 8.57–8.58 (m, 1H, Pyridine-H), 9.05 (s, 1H, CONHAr), 9.16 (t, 1H, ^3J = 5.6 Hz, CON$\underline{H}$CH$_2$), 13.03 (d, 1H, ^4J = 2.0 Hz, Pyrr-NH). ^{13}C NMR (100 MHz, DMSO-d6) δ 21.75 (CH($\underline{C}H_3$)$_2$), 44.72 (CH$_2$), 71.29 ($\underline{C}H$(CH$_3$)$_2$), 98.43, 106.30, 112.77, 113.83, 119.75, 120.96, 122.08, 122.60, 127.60, 130.39, 130.51, 136.72, 148.31, 148.82, 157.02, 158.84, 165.68 (Ar-$\underline{C}$ONH). MS (ESI) m/z = 533.0 ([M-H]$^-$), HRMS for C$_{21}$H$_{19}$Br$_2$N$_4$O$_3$: calculated 532.9824, found 532.9834. HPLC: t_r 8.831 min (98.9% at 280 nm, method A).

4.8.10.6 Methyl 2-hydroxy-4-nitrobenzoate (17): Synthesized according to General procedure A without purification with petroleum ether. The starting compound (**16,** 5.00 g, 25.7 mmol) was dissolved from the begining. Yellow solid; yield 89% (4.80 g); mp 97–99 °C (101–102 °C, lit [42]). IR (ATR) ν = 3114, 2961, 2868, 1676, 1519, 1434, 1339, 1250, 1197, 1070, 957, 902, 812, 786, 732 cm^{-1}. ^{1}H NMR (400 MHz, CDCl$_3$) δ 4.05 (s, 3H, COOCH$_3$), 7.73 (dd, 1H, ^3J = 8.8 Hz, ^4J = 2.4 Hz, Ar-H-5), 7.85 (d, 1H, ^4J = 2.4 Hz, Ar-H-3), 8.05 (d, 1H, ^3J = 8.4 Hz, Ar-H-6), 11.01 (s, 1H, OH).

4.8.10.7 Methyl 2-(benzyloxy)-4-nitrobenzoate (18a) [43]: To a solution of methyl 2-hydroxy-4-nitrobenzoate (**17,** 1.00 g, 5.06 mmol) and potassium carbonate (1.40 g, 10.1 mmol) in acetonitrile (40 mL) benzyl bromide (0.60 mL, 5.06 mmol) was added and the reaction mixture was stirred at 60°C for 15 h. The solvent was evaporated under reduced pressure, the residue was dissolved in ethyl acetate (40 mL) and water (40 mL), the organic phase was washed with brine (2 × 30 mL), dried over Na$_2$SO$_4$, filtered and the solvent removed under reduced pressure to give **18a** (1.24 g) as yellow solid. Yield 85% (1.24g); mp 74–76°C; ^{1}H NMR (400 MHz, CDCl$_3$) δ 3.97 (s, 3H, COOCH$_3$), 5.30 (s, 2H, CH$_2$), 7.35–7.54 (m, 5H, 5 × Ar-H), 7.86–7.96 (m, 2H, 3 × Ar-H).

4.8.10.8   2-(Benzyloxy)-4-nitrobenzoic acid (19a) [43]: Synthesized according to General procedure C. Yellow solid; yield 87% (1.02 g); mp 151–153 °C. IR (ATR) ν = 3061, 2941, 2865, 2648, 2537, 1678, 1522, 1345, 1244, 1082, 988, 949, 875, 811, 734 cm^{-1}. ^{1}H NMR(400 MHz, CDCl$_3$) δ 5.42 (s, 2H, CH$_2$), 7.45–7.52 (m, 5H, 5 × Ar-H′), 8.00 (dd, 1H, ^{3}J = 8.4 Hz, ^{4}J = 2.0 Hz, Ar-H-5), 8.03 (d, 1H, ^{4}J = 2.0 Hz, Ar-H-3), 8.38 (d, 1H, ^{3}J = 8.4 Hz, Ar-H-6), 10.56 (br s, 1H, COOH).

4.8.10.9   Methyl (2-(benzyloxy)-4-nitrobenzoyl)glycinate (20a): Synthesized according to General procedure D with 2-(benzyloxy)-4-nitrobenzoic acid (**19a,** 1.00 g, 3.64 mmol) and glycine methyl ester hydrochloride (505 mg, 4.03 mmol) as reagents. The crude product was purified by adding petroleum ether, the obtained suspension was sonicated, filtered and washed with petroleum ether to give **20a** (1.18 g) as yellow solid. Yield 85% (1.18 g); mp 119–122 °C. IR (ATR) ν = 3367, 3105, 2950, 2855, 1750, 1648, 1518, 1442, 1342, 1202, 1101, 989, 923, 838, 743 cm^{-1}. ^{1}H NMR (400 MHz, DMSO-d6) δ 3.66 (s, 1H, COOCH$_3$), 4.08 (d, 2H, ^{3}J = 6.0 Hz, CONHC$\underline{H}_2$), 5.44 (s, 2H, OCH$_2$Ph), 7.32–7.54 (m, 5H, 5 × Ar-H′), 7.85 (d, 1H, ^{3}J = 8.4 Hz, Ar-H-6), 7.91 (dd, 1H, ^{3}J = 8.4 Hz, ^{4}J = 2.0 Hz, Ar-H-5), 7.98 (d, 1H, ^{4}J = 2.0 Hz, Ar-H-3), 8.90 (t, 1H, ^{3}J = 6.0 Hz, CONHC$\underline{H}_2$). ^{13}C NMR (100 MHz, DMSO-d6) δ 41.25 (CH$_2$), 51.81 (COOC$\underline{H}_3$), 70.35 (CH$_2$), 108.46, 115.68, 127.33, 128.01, 128.52, 130.03, 131.09, 135.90, 149.35, 155.98, 164.44 (CONH), 169.93 ($\underline{C}$OOCH$_3$). MS (ESI) m/z = 367.32 ([M+Na]$^+$).

4.8.10.10   Methyl (4-amino-2-(benzyloxy)benzoyl)glycinate (21a): A mixture of compound **20a** (675 mg, 1.98 mmol) and SnCl$_2$ (1.85 g, 16.9 mmol) in ethyl acetate (20 mL) and methanol (20 mL) was stirred at 55 °C for 15 h. The solvent was removed under reduced pressure and the residue dissolved in ethyl acetate (20 mL) and water (20 mL). The aqueous phase was basified with 1 M NaOH to pH 9 and extracted with ethyl acetate (2 × 20 mL). The combined organic phases were dried over Na$_2$SO$_4$, filtered and the solvent evaporated under reduced pressure. The crude product was purified with flash column chromatography using ethyl acetate/petroleum ether (2/1) as an eluent to give compound **21a** (356 mg) as yellow oil. Yield 58% (356 mg). IR (ATR) ν = 3378, 3335, 3232, 2953, 1737, 1596, 1539, 1440, 1281, 1198, 1118, 1005, 825, 732 cm^{-1}. ^{1}H NMR (400 MHz, CDCl$_3$) δ 3.70 (s, 1H, COOCH$_3$), 4.16 (d, 2H, ^{3}J = 5.6 Hz, CONHC$\underline{H}_2$), 4.33 (br s, 2H, NH$_2$), 5.17 (s, 2H, C$\underline{H}_2$Ph), 6.31 (d, 1H, ^{4}J = 2.0 Hz, Ar-H-3), 6.38 (dd, 1H, ^{3}J = 8.4 Hz, ^{4}J = 2.0 Hz, Ar-H-5), 7.35–7.48 (m, 5H, 5 × Ar-H′), 8.04 (d, 1H, ^{3}J = 8.8 Hz, Ar-H-6), 8.29 (t, 1H, ^{3}J = 4.4 Hz, CONHC$\underline{H}_2$). ^{13}C NMR (100 MHz, DMSO-d6) δ 41.20 (CH$_2$), 51.64 (COOC$\underline{H}_3$), 69.39 (CH$_2$), 97.31, 106.47, 108.42, 127.34, 127.88, 128.51, 132.73, 136.61, 153.44, 158.06, 165.05 (CONH), 170.69 ($\underline{C}$OOCH$_3$). MS (ESI) m/z = 337.33 ([M+Na]$^+$).

4.8.10.11   Methyl (2-(benzyloxy)-4-(4,5-dibromo-1H-pyrrole-2-carboxamido)benzoyl)glycinate (22a): Synthesized according to General procedure F. The crude product was purified by adding diethyl ether (15 mL) and methanol (5 mL), the obtained suspension was sonicated, filtered and washed with diethyl ether (2 × 10 mL) to obtain **22a** (192 mg) as white solid. Yield 34% (192 mg); mp 103–106°C. IR (ATR) ν = 3421, 3370, 3306, 3129, 1736, 1627, 1593, 1520, 1332, 1217, 1076, 979, 836, 740 cm^{-1}. ^{1}H NMR (400 MHz, DMSO-d6) δ 3.65 (s, 3H, COOCH$_3$), 4.08 (d, 2H, ^{3}J = 6.0 Hz,

CON<u>H</u>C<u>H</u>₂), 5.34 (s, 2H, OC<u>H</u>₂Ph), 7.27 (d, 1H, ^4J = 2.8 Hz, Pyrr-CH), 7.32–7.42 (m, 4H, 4 × Ar-H), 7.52–7.54 (m, 2H, 2 × Ar-H), 7.77–7.86 (m, 2H, 2 × Ar-H), 8.58 (t, 1H, ^3J = 6.0 Hz, CON<u>H</u>CH₂), 10.05 (s, 1H, Pyrr-CON<u>H</u>-Ar), 13.01 (d, 1H, ^4J = 2.4 Hz, Pyrr-NH); ^{13}C NMR (100 MHz, DMSO-d6) δ 41.26 (CH₂), 51.65 (COO<u>C</u>H₃), 69.74 (CH₂), 98.19, 104.16, 106.53, 111.74, 114.17, 116.57, 127.34, 127.46, 127.90, 128.44, 131.58, 136.14, 142.86, 156.49, 157.39, 164.48 (Ar-<u>C</u>ONH), 170.29 (<u>C</u>OOCH₃). MS (ESI) m/z = 562.0 ([M-H]$^-$), HRMS for C₂₂H₁₈Br₂N₃O₅: calculated 561.9613, found 561.9606. HPLC: t_r 12.252 min (95.1% at 280 nm, method A).

4.8.10.12   (2-(Benzyloxy)-4-(4,5-dibromo-1H-pyrrole-2-carboxamido)benzoyl)glycine (23a): Synthesized according to General procedure G with 2 equivalents of 1 M NaOH (140 μL, 140 μmol). White solid; yield 46% (18 mg); mp 195–198 °C. IR (ATR) ν = 3369, 3222, 2930, 1714, 1618, 1510, 1408, 1294, 1205, 1119, 1019, 842, 737 cm^{-1}. ^{1}H NMR (400 MHz, DMSO-d6) δ 4.00 (d, 2H, ^3J = 5.6 Hz, CONHC<u>H</u>₂), 5.33 (s, 2H, C<u>H</u>₂Ph), 7.26 (s, 1H, Pyrr-CH), 7.30–7.55 (m, 6H, 5 × Ar-H′, Ar-H-5), 7.77 (d, 1H, ^4J = 2.0 Hz, Ar-H-3), 7.87 (d, 1H, ^3J = 8.4 Hz, Ar-H-6), 8.49 (t, 1H, ^3J = 5.6 Hz, CON<u>H</u>CH₂), 10.03 (s, 1H, Pyrr-CON<u>H</u>-Ar), 12.68 (br s, 1H, COOH/Pyrr-NH), 13.00 (br s, 1H, COOH/Pyrr-NH); ^{13}C NMR (100 MHz, DMSO-d6) δ 41.32 (CH₂), 69.84 (CH₂), 98.18, 104.16, 106.53, 111.75, 114.17, 116.62, 127.44, 127.48, 127.93, 128.43, 131.63, 136.07, 142.82, 156.51, 157.40, 164.23 (Ar-<u>C</u>ONH), 171.21 (<u>C</u>OOH). MS (ESI) m/z = 547.9 ([M-H]$^-$), HRMS for C₂₁H₁₆Br₂N₃O₅: calculated 547.9457, found 547.9454. HPLC: t_r 10.497 min (97.5% at 280 nm, method A).

Supplementary Material

Refer to Web version on PubMed Central for supplementary material.

Acknowledgment

Abbreviations

ATCC   American type culture collection

ATR   attenuated total reflectance

CDI	1,1′-carbonyldiimidazole
CFU	colony-forming unit
CLSI	Clinical and Laboratory Standards Institute
DIAD	diisopropyl azodicarboxylate
DTT	dithiothreitol
FBS	fetal bovine serum
GyrA	DNA gyrase A
GyrB	DNA gyrase B
HepG2	human hepatocellular carcinoma cell line
HUVEC	human umbilical vein endothelial cells
MH	Mueller Hinton
MRSA	methicillin-resistant *Staphylococcus aureus*
MTS	3-(4,5-dimethylthiazol-2-yl)-5-(3-carboxymethoxyphenyl)-2-(4-sulfophenyl)-2*H*-tetrazolium
NMM	*N*-methylmorpholine
ParC	topoisomerase IV subunit A
ParE	topoisomerase IV subunit B
PAβN	phenylalanine-arginine β-naphthylamide
RA	residual activity
TBTU	*N,N,N′,N′*-tetramethyl-*O*-(benzotriazol-1-yl)uronium tetrafluoroborate
topo IV	topoisomerase IV
VRE	vancomycin-resistant *Enterococci*

References

[1]. Klahn P, Bronstrup M. New structural templates for clinically validated and novel targets in antimicrobial drug research and development. Curr Top Microbiol Immunol. 2016; 398:365–417. [PubMed: 27704270]

[2]. Chan PF, Germe T, Bax BD, Huang J, Thalji RK, Bacque E, Checchia A, Chen D, Cui H, Ding X, Ingraham K, et al. Thiophene antibacterials that allosterically stabilize DNA-cleavage complexes with DNA gyrase. Proc Natl Acad Sci U S A. 2017; 114:4492–4500.

[3]. Boucher HW, Talbot GH, Bradley JS, Edwards JE, Gilbert D, Rice LB, Scheld M, Spellberg B, Bartlett J. Bad bugs, no drugs: no ESKAPE! an update from the Infectious Diseases Society of America. Clin Infect Dis. 2009; 48:1–12. [PubMed: 19035777]

[4]. World Health Organisation. [Accessed 30 September 2017] Global priority list of antibiotic-resistant to guide research, discovery, and development of new antibiotics. 2017. Available at,

http://www.who.int/medicines/publications/WHO-PPL-Short_Summary_ 25Feb-ET_NM_WHO.pdf

[5]. Collin F, Karkare S, Maxwell A. Exploiting bacterial DNA gyrase as a drug target: current state and perspectives. Appl Microbiol Biotechnol. 2011; 92:479–497. [PubMed: 21904817]

[6]. Tomaši T, Maši LP. Prospects for developing new antibacterials targeting bacterial type IIA topoisomerases. Curr Top Med Chem. 2014; 14:130–151. [PubMed: 24236722]

[7]. Champoux JJ. DNA topoisomerases: structure, function, and mechanism. Annu Rev Biochem. 2001; 70:369–413. [PubMed: 11395412]

[8]. Oblak M, Kotnik M, Solmajer T. Discovery and development of ATPase inhibitors of DNA gyrase as antibacterial agents. Curr Med Chem. 2007; 14:2033–2047. [PubMed: 17691945]

[9]. Savage VJ, Charrier C, Salisbury AM, Moyo E, Forward H, Chaffer-Malam N, Metzger R, Huxley A, Kirk R, Uosis-Martin M, Noonan G, et al. Biological profiling of novel tricyclic inhibitors of bacterial DNA gyrase and topoisomerase IV. J Antimicrob Chemother. 2016; 71:1905–1913. [PubMed: 27032669]

[10]. Azam MA, Thathan J, Jubie S. Dual targeting DNA gyrase B (GyrB) and topoisomerse IV (ParE) inhibitors: a review. Bioorg Chem. 2015; 62:41–63. [PubMed: 26232660]

[11]. Bisacchi GS, Manchester JI. A new-class antibacterial-almost. Lessons in drug discovery and development: a critical analysis of more than 50 years of effort toward ATPase inhibitors of DNA gyrase and topoisomerase IV. ACS Infect Dis. 2015; 1:4–41. [PubMed: 27620144]

[12]. Silver LL. A gestalt approach to Gram-negative entry. Bioorg Med Chem. 2016; 24:6379–6389. [PubMed: 27381365]

[13]. Gjorgjieva M, Tomaši T, Baran oková M, Katsamakas S, Ilaš J, Tammela P, Peterlin Maši L, Kikelj D. Discovery of benzothiazole scaffold-based DNA gyrase B inhibitors. J Med Chem. 2016; 59:8941–8954. [PubMed: 27541007]

[14]. Trzoss M, Bensen DC, Li X, Chen Z, Lam T, Zhang J, Creighton CJ, Cunningham ML, Kwan B, Stidham M, Nelson K, et al. Pyrrolopyrimidine inhibitors of DNA gyrase B (GyrB) and topoisomerase IV (ParE), Part II: development of inhibitors with broad spectrum, Gram-negative antibacterial activity. Bioorg Med Chem Lett. 2013; 23:1537–1543. [PubMed: 23294697]

[15]. Zhang J, Yang Q, Romero JA, Cross J, Wang B, Poutsiaka KM, Epie F, Bevan D, Wu Y, Moy T, Daniel A, et al. Discovery of indazole derivatives as a novel class of bacterial gyrase B inhibitors. ACS Med Chem Lett. 2015; 6:1080–1085. [PubMed: 26487916]

[16]. Durcik M, Tammela P, Baran oková M, Tomaši T, Ilaš J, Kikelj D, Zidar N. Synthesis and evaluation of N-phenylpyrrolamides as DNA gyrase B inhibitors. ChemMedChem. 2017; 5 201700549.

[17]. Tari LW, Li X, Trzoss M, Bensen DC, Chen Z, Lam T, Zhang J, Lee SJ, Hough G, Phillipson D, Akers-Rodriguez S, et al. Tricyclic GyrB/ParE (TriBE) inhibitors: a new class of broad-spectrum dual-targeting antibacterial agents. PLoS One. 2013; 8:e84409. [PubMed: 24386374]

[18]. Zhang J, Yang Q, Cross JB, Romero JA, Poutsiaka KM, Epie F, Bevan D, Wang B, Zhang Y, Chavan A, Zhang X, et al. Discovery of azaindole ureas as a novel class of bacterial gyrase B inhibitors. J Med Chem. 2015; 58:8503–8512. [PubMed: 26460684]

[19]. Richter MF, Drown BS, Riley AP, Garcia A, Shirai T, Svec RL, Hergenrother PJ. Predictive compound accumulation rules yield a broad - spectrum antibiotic. Nature. 2017; 545:299–304. [PubMed: 28489819]

[20]. Basarab GS, Manchester JI, Bist S, Boriack-Sjodin PA, Dangel B, Illingworth R, Sherer BA, Sriram S, Uria-Nickelsen M, Eakin AE. Fragment-to-hit-to-lead discovery of a novel pyridylurea scaffold of ATP competitive dual targeting type II topoisomerase inhibiting antibacterial agents. J Med Chem. 2013; 56:8712–8735. [PubMed: 24098982]

[21]. Lassalas P, Gay B, Lasfargeas C, James MJ, Tran V, Vijayendran KG, Brunden KR, Kozlowski MC, Thomas CJ, Smith AB 3rd, Huryn DM, et al. Structure property relationships of carboxylic acid isosteres. J Med Chem. 2016; 59:3183–3203. [PubMed: 26967507]

[22]. Brvar M, Perdih A, Renko M, Anderluh G, Turk D, Solmajer T. Structure-based discovery of substituted 4,5'-bithiazoles as novel DNA gyrase inhibitors. J Med Chem. 2012; 55:6413–6426. [PubMed: 22731783]

[23]. Barrish JC, Gordon E, Alam M, Lin PF, Bisacchi GS, Chen P, Cheng PTW, Fritz AW, Greytok JA, Hermsmeier MA, Humphreys WG, et al. Aminodiol HIV protease inhibitors .1. Design, synthesis, and preliminary SAR. J Med Chem. 1994; 37:1758–1768. [PubMed: 8021916]

[24]. PyMOL. Delano Scientific LLC; San Francisco, CA: http://pymol.sourceforge.net

[25]. Tomaši T, Katsamakas S, Hodnik Z, Ilaš J, Brvar M, Solmajer T, Montalvão S, Tammela P, Banjanac M, Ergovi G, Anderluh M, et al. Discovery of 4,5,6,7-tetrahydrobenzo[1,2-d]thiazoles as novel DNA gyrase inhibitors targeting the ATP-binding site. J Med Chem. 2015; 58:5501–5521. [PubMed: 26098163]

[26]. Zidar N, Macut H, Tomaši T, Brvar M, Montalvão S, Tammela P, Solmajer T, Peterlin Maši L, Ilaš J, Kikelj D. N-Phenyl-4,5-dibromopyrrolamides and N-phenylindolamides as ATP competitive DNA gyrase B inhibitors: design, synthesis, and evaluation. J Med Chem. 2015; 58:6179–6194. [PubMed: 26126187]

[27]. Baker KR, Jana B, Franzyk H, Guardabassi L. A high-throughput approach to identify compounds that impair envelope integrity in Escherichia coli. Antimicrob Agents Chemother. 2016; 60:5995–6002. [PubMed: 27458225]

[28]. Tillotson G. A crucial list of pathogens. Lancet Infect Dis. 2017; :30754–30755. DOI: 10.1016/S1473-3099(17)

[29]. Stokes JM, MacNair CR, Ilyas B, French S, Cote JP, Bouwman C, Farha MA, Sieron AO, Whitfield C, Coombes BK, Brown ED. Pentamidine sensitizes Gram-negative pathogens to antibiotics and overcomes acquired colistin resistance. Nat Microbiol. 2017; 2

[30]. Baba T, Ara T, Hasegawa M, Takai Y, Okumura Y, Baba M, Datsenko KA, Tomita M, Wanner BL, Mori H. Construction of Escherichia coli K-12 inframe, single-gene knockout mutants: the Keio collection. Mol Syst Biol. 2006; 2

[31]. ISO 20776–1:2006-Clinical laboratory testing and in vitro diagnostic test systems – Susceptibility testing of infectious agents and evaluation of performance of antimicrobial susceptibility test devices – Part 1: Reference method for testing the in vitro activity of antimicrobial agents against rapidly growing aerobic bacteria involved in infectious diseases. ISO; http://www.iso. org/iso/catalogue_detail.htm?csnumber=41630

[32]. Garg G, Zhao H, Blagg BS. Design, synthesis, and biological evaluation of ring-constrained novobiocin analogues as Hsp90 C-terminal inhibitors. ACS Med Chem Lett. 2015; 6:204–209. [PubMed: 25699150]

[33]. Promega Corporation; Madison, WI: https://worldwide.promega.com/

[34]. Pingeaw R, Mandi P, Nantasenamat C, Prachayasittikul S, Ruchirawat S, Prachayasittikul V. Design, synthesis and molecular docking studies of novel N-benzenesulfonyl-1,2,3,4-tetrahydroisoquinoline-based triazoles with potent anticancer activity. Eur J Med Chem. 2014; 81:192–203. [PubMed: 24836071]

[35]. Budovská M, Pilátová M, Varinská L, Mojžiš J, Mezencev R. The synthesis and anticancer activity of analogs of the indole phytoalexins brassinin, 1-methoxyspirobrassinol methyl ether and cyclobrassinin. Bioorg Med Chem. 2013; 21:6623–6633. [PubMed: 24012378]

[36]. GraphPad Software. San Diego, CA: https://www.graphpad.com/

[37]. GAMESS interface, Chem3D 16.0, ChemOffice Professional 16.0 Suite, CambridgeSoft

[38]. Halgren TA. Merck molecular force field .1. Basis, form, scope, parameterization, and performance of MMFF94. J Comput Chem. 1996; 17:490–519.

[39]. Jones G, Willett P, Glen RC, Leach AR, Taylor R. Development and validation of a genetic algorithm for flexible docking. J Mol Biol. 1997; 267:727–748. [PubMed: 9126849]

[40]. Ekici OD, Li ZZ, Campbell AJ, James KE, Asgian JL, Mikolajczyk J, Salvesen GS, Ganesan R, Jelakovic S, Grutter MG, Powers JC. Design, synthesis, and evaluation of aza-peptide Michael acceptors as selective and potent inhibitors of caspases-2, -3, -6, -7, -8, -9, and -10. J Med Chem. 2006; 49:5728–5749. [PubMed: 16970398]

[41]. Plante J, Campbell F, Malkova B, Kilner C, Warriner SL, Wilson AJ. Synthesis of functionalised aromatic oligamide rods. Org Biomol Chem. 2008; 6:138–146. [PubMed: 18075658]

[42]. Wilder Smith AE, Frommel E. The preparation of some 1,3,4-oxadiazol-2-ols and oxadiazol-2-thiols active as tuberculostatics. Arzneimittelforschung. 1962; 12:485–487. [PubMed: 14006977]

[43]. Prabhakaran P, Azzarito V, Jacobs T, Hardie MJ, Kilner CA, Edwards TA, Warriner SL, Wilson AJ. Conformational properties of *O*-alkylated benzamides. Tetrahedron. 2012; 68:4485–4491.
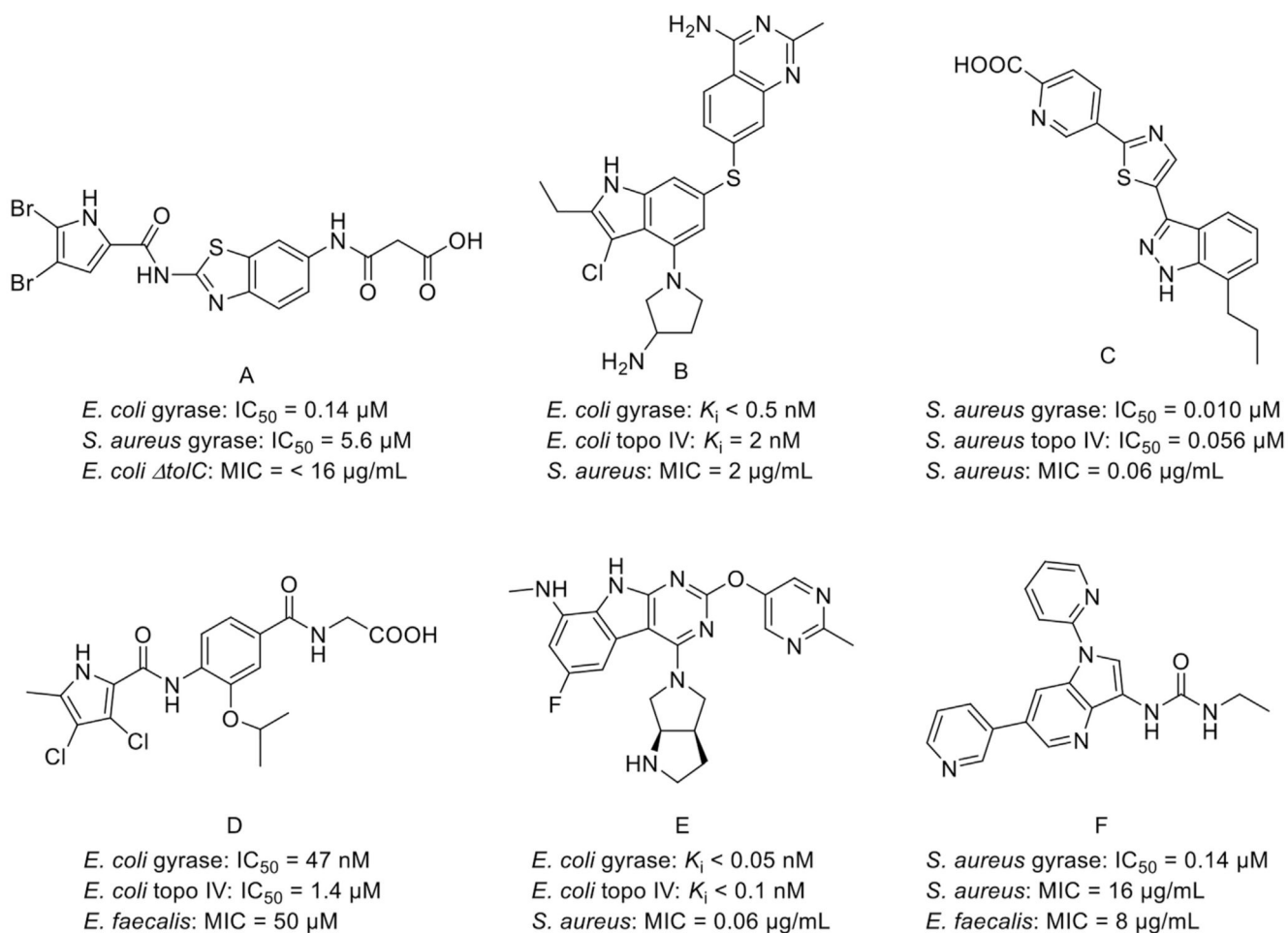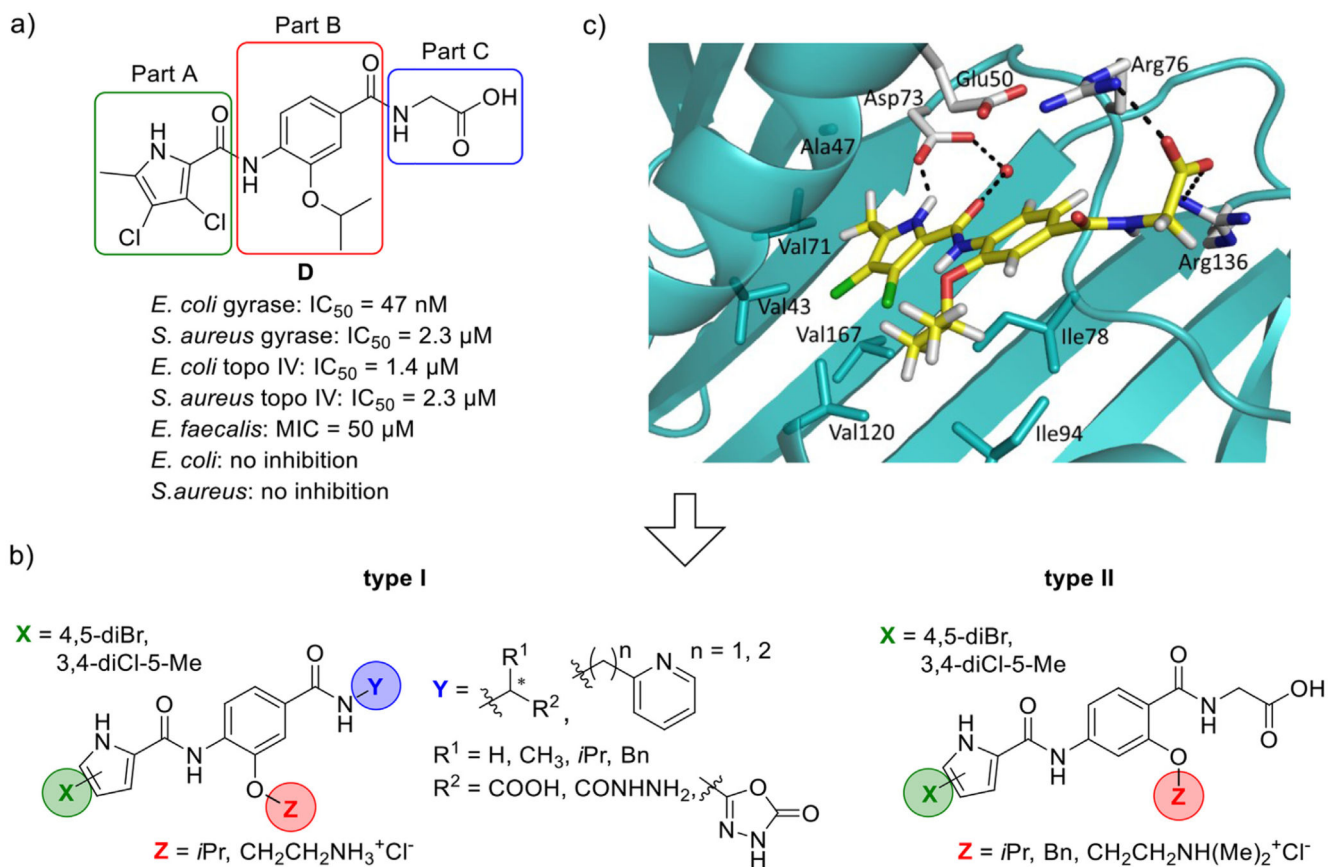
Fig. 1.

Representative DNA gyrase B inhibitors: benzothiazole A [13], pyrrolopyrimidine B [14], indazole C [15], pyrrolamide D [16], pyrimidoindole E [17], azaindole urea F [18], and their IC_{50} or K_i, and MIC values.

Fig. 2.

a) A representative *N*-phenylpyrrolamide D and its inhibitory activities on DNA gyrase and topoisomerase IV [16]; b) Structures of type I and type II *N*-phenylpyrrolamide inhibitors; c) Docking binding mode of inhibitor D coloured according to the atom chemical type (C, yellow; N, blue; O, red; Cl, green) in the ATP binding site of *E. coli* GyrB (in cyan, PDB code: 4DUH [22]). The water molecule is presented as a red sphere. (For interpretation of the references to colour in this figure legend, the reader is referred to the Web version of this article.)
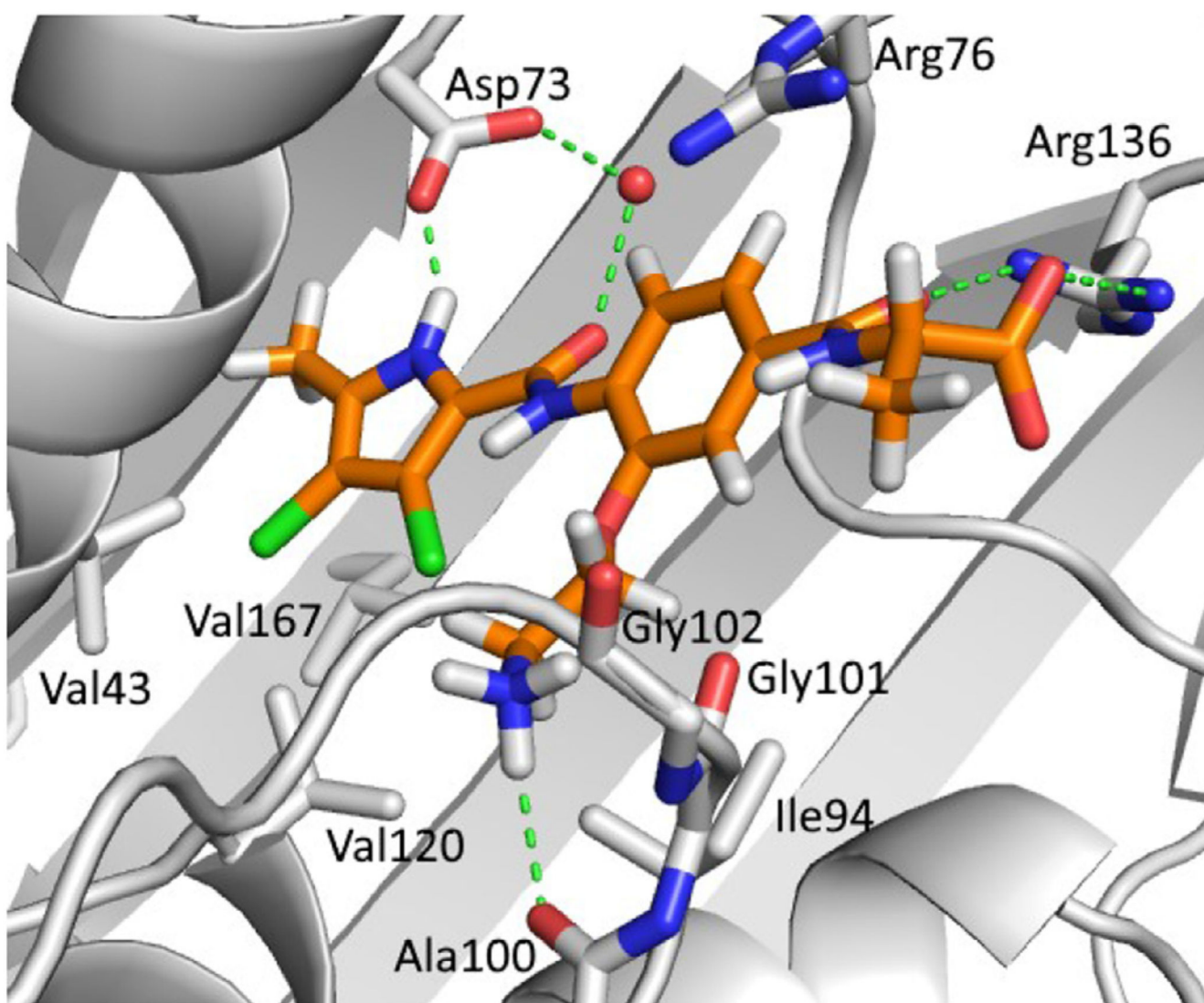
Fig. 3.
The GOLD-predicted binding pose of inhibitor **9e** (in orange sticks) in the *E. coli* GyrB
ATP-binding site (PDB entry: 4DUH [22], in grey). Hydrogen bonds are presented as green
dashed lines. The water molecule is shown as a red sphere. The figure was prepared with
PyMOL [24]. (For interpretation of the references to colour in this figure legend, the reader
is referred to the Web version of this article.)
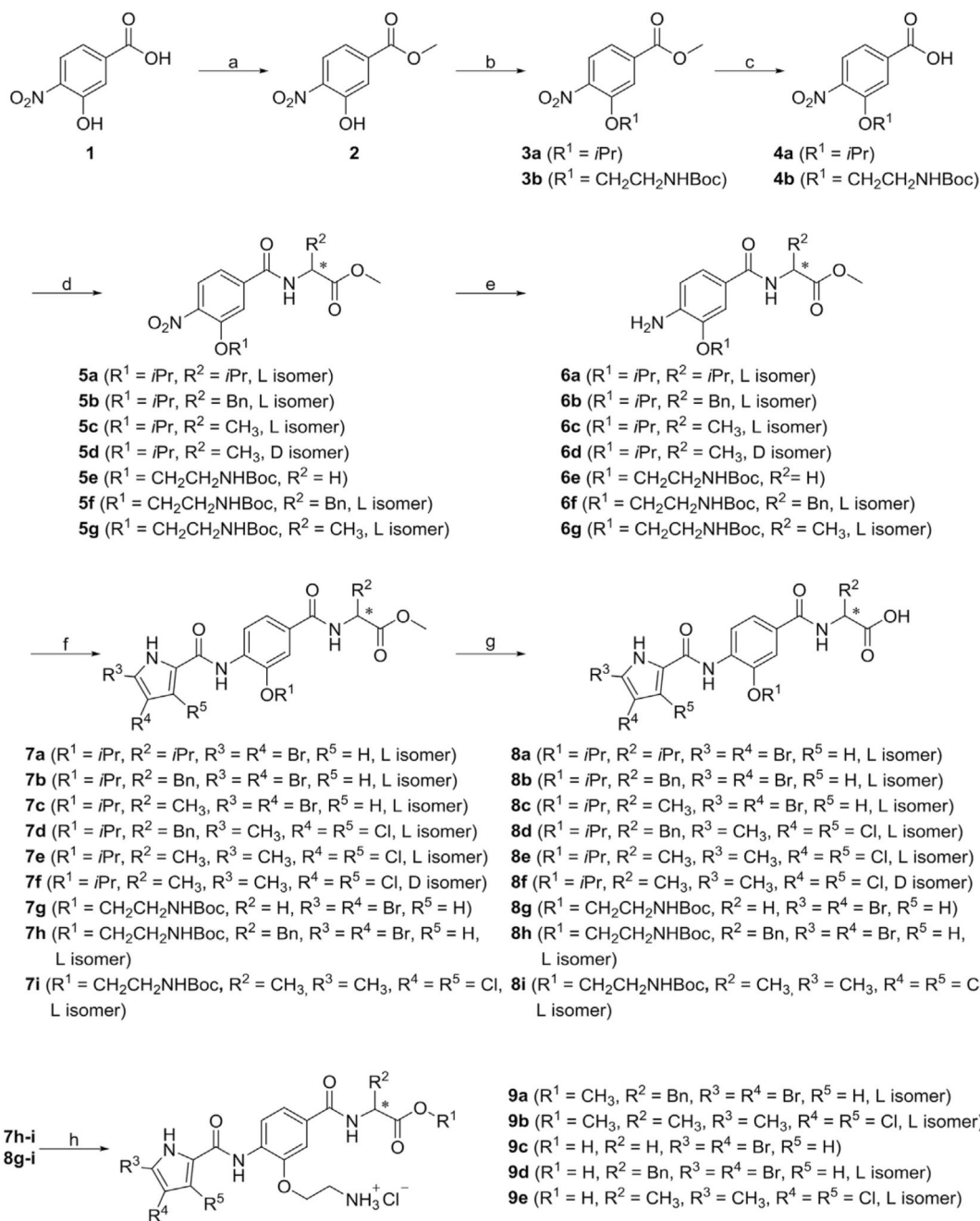
Scheme 1.

Reagents and conditions: (a) thionyl chloride, MeOH, 0 °C → rt, 15 h; (b) isopropanol, triphenylphosphine, diisopropyl azodicarboxylate, THF, rt, 15 h (for the synthesis of **3a**), *tert*-butyl (2-chloroethyl)carbamate, K_2CO_3, KI, DMF, rt → 60 °C, 15 h (for the synthesis of **3b**); (c) 1 M NaOH, MeOH, rt, 15 h; (d) corresponding amino acid methyl ester hydrochloride, TBTU, NMM, CH_2Cl_2, rt, 15 h; (e) H_2, Pd-C, MeOH, rt, 2–4 h; (f) corresponding pyrrole carboxylic acid, oxalyl chloride, CH_2Cl_2, rt, 15 h, then *ii*) **6a-g,** pyridine, CH_2Cl_2, rt, 15 h; (g) 1 M NaOH, MeOH/THF, rt, 15 h (for the synthesis of **8a-e**

and **8g-i**) or 1 M LiOH, MeOH/THF, rt, 4 h (for the synthesis of **8f**); (h) 4 M HCl in 1,4-dioxane, THF, rt, 2 h.
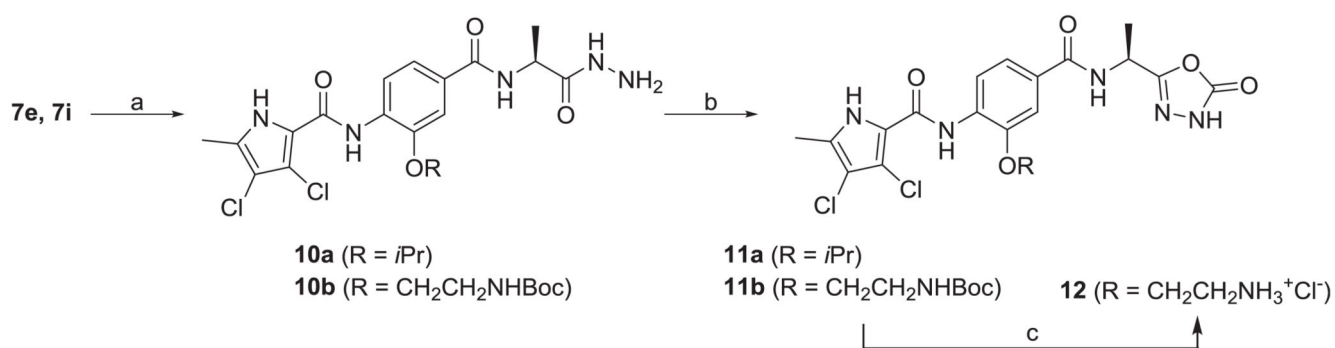
Scheme 2.
Reagents and conditions: (a) hydrazine monohydrate, MeOH/THF, 65 °C, 15 h (for the synthesis of **10a**) or 4 d (for the synthesis of **10b**); (b) CDI, 1,4-dioxane/DMF, 100 °C, 15 h; (c) 4 M HCl in 1,4-dioxane, THF, rt, 5 h.
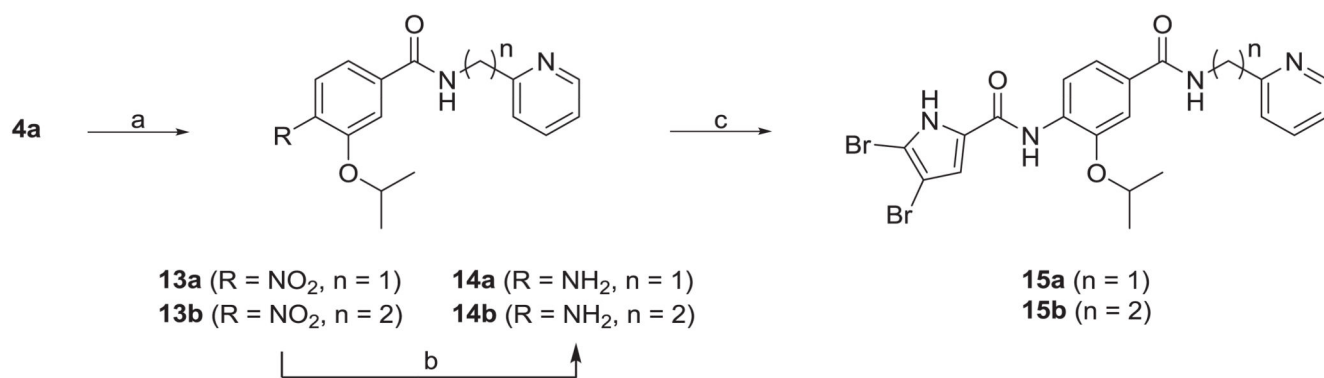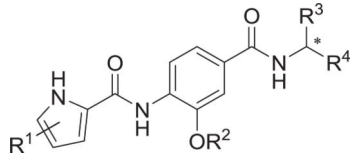
Scheme 3.
Reagents and conditions: (a) pyridin-2-ylmethanamine (for the synthesis of **13a**) or 2-(pyridin-2-yl)ethan-1-amine (for the synthesis of **13b**), TBTU, NMM, CH_2Cl_2, rt, 15 h; (b) H_2, Pd-C, MeOH, rt, 5 h; (c) 4,5-dibromopyrrole-2-carboxylic acid, oxalyl chloride, CH_2Cl_2, rt, 15 h, then *ii*) **14a-b,** pyridine, CH_2Cl_2, rt, 15 h.
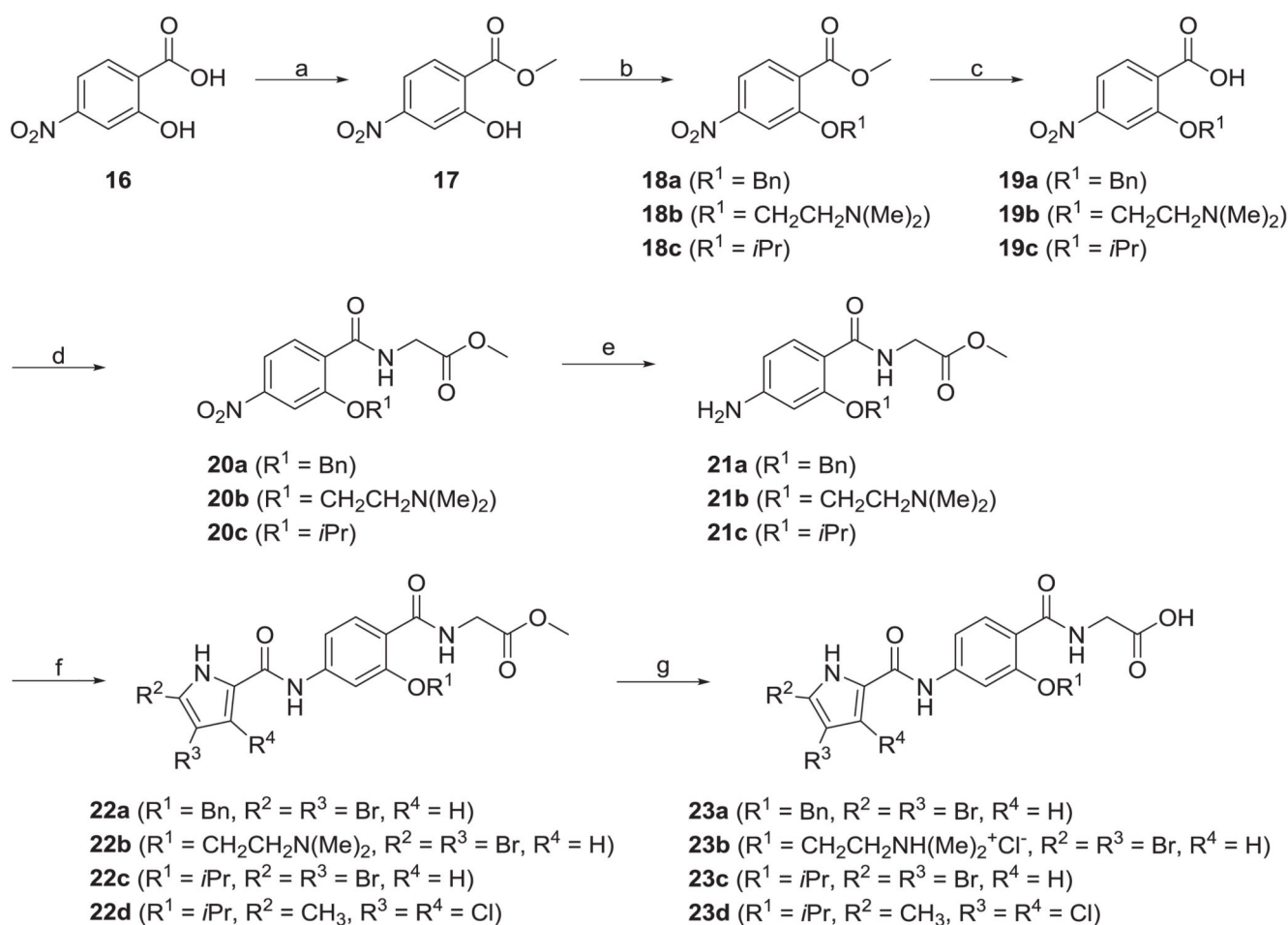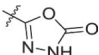
Scheme 4.
Reagents and conditions: (a) thionyl chloride, MeOH, 0 °C / rt, 15 h; (b) K$_2$CO$_3$, benzyl bromide, CH$_3$CN, 60 °C, 15 h (for the synthesis of **18a**), *β*-dimethyl-amino-ethylchloride hydrochloride, K$_2$CO$_3$, THF, 60 °C, 72 h (for the synthesis of **18b**), isopropanol, triphenylphospine, DIAD, THF, rt, 15 h (for the synthesis of **18c**); (c) 1 M NaOH, MeOH, rt, 15 h; (d) glycine methyl ester hydrochloride, TBTU, NMM, CH$_2$Cl$_2$, rt, 15 h; (e) SnCl$_2$, EtOAc/MeOH, 55 °C, 15 h (for the synthesis of **21a**), H$_2$, Pd-C, MeOH, rt, 3 h, (for the synthesis of **21b-c**); (f) the corresponding pyrrole carboxylic acid, oxalyl chloride, CH$_2$Cl$_2$, rt, 15 h, then *ii)* **21a-c,** pyridine, CH$_2$Cl$_2$, rt, 15 h; (g) 1 M NaOH, MeOH/THF, rt, 15 h.

Table 1

Inhibitory activity of type I compounds **7a-i, 8a-i, 9a-e, 10a-b, 11a-b, 12** and **15a-b** against DNA gyrase from *E. coli.*
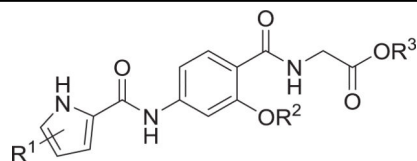

Compd.	R^1	R^2	R^3	R^4	*	IC_{50} (nM)^a or RA (%)^b
						E. coli gyrase
7a	4,5-diBr	iPr	iPr	COOMe	L	94%
7b	4,5-diBr	iPr	Bn	COOMe	L	100%
7c	4,5-diBr	iPr	CH$_3$	COOMe	L	93%
7d	3,4-diCl-5-Me	iPr	Bn	COOMe	L	100%
7e	3,4-diCl-5-Me	iPr	CH$_3$	COOMe	L	66%
7f	3,4-diCl-5-Me	iPr	CH$_3$	COOMe	D	87%
7g	4,5-diBr	CH$_2$CH$_2$NHBoc	H	COOMe	/	53%
7h	4,5-diBr	CH$_2$CH$_2$NHBoc	Bn	COOMe	L	100%
7i	3,4-diCl-5-Me	CH$_2$CH$_2$NHBoc	CH$_3$	COOMe	L	100%
8a	4,5-diBr	iPr	iPr	COOH	L	70%
8b	4,5-diBr	iPr	Bn	COOH	L	100%
8c	4,5-diBr	iPr	CH$_3$	COOH	L	370 ± 160 nM
8d	3,4-diCl-5-Me	iPr	Bn	COOH	L	91%
8e	3,4-diCl-5-Me	iPr	CH$_3$	COOH	L	38 ± 9 nM
8f	3,4-diCl-5-Me	iPr	CH$_3$	COOH	D	41 ± 16 nM
8g	4,5-diBr	CH$_2$CH$_2$NHBoc	H	COOH	/	96%
8h	4,5-diBr	CH$_2$CH$_2$NHBoc	Bn	COOH	L	100%
8i	3,4-diCl-5-Me	CH$_2$CH$_2$NHBoc	CH$_3$	COOH	L	590 ± 20 nM
9a	4,5-diBr	CH$_2$CH$_2$NH$_3^+$Cl$^-$	Bn	COOMe	L	85%
9b	3,4-diCl-5-Me	CH$_2$CH$_2$NH$_3^+$Cl$^-$	CH$_3$	COOMe	L	34 ± 1 nM
9c	4,5-diBr	CH$_2$CH$_2$NH$_3^+$Cl$^-$	H	COOH	L	50%
9d	4,5-diBr	CH$_2$CH$_2$NH$_3^+$Cl$^-$	Bn	COOH	L	370 ± 10 nM
9e	3,4-diCl-5-Me	CH$_2$CH$_2$NH$_3^+$Cl$^-$	CH$_3$	COOH	L	28 ± 7 nM
10a	3,4-diCl-5-Me	iPr	CH$_3$	CONHNH$_2$	L	280 ± 80 nM
10b	3,4-diCl-5-Me	CH$_2$CH$_2$NHBoc	CH$_3$	CONHNH$_2$	L	68%
11a	3,4-diCl-5-Me	iPr	CH$_3$		L	85 ± 7 nM
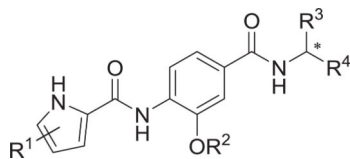
Compd.	R¹	R²	R³	R⁴	*	IC₅₀ (nM)[a] or RA (%)[b] *E. coli* gyrase
11b	3,4-diCl-5-Me	CH_2CH_2NHBoc	CH_3		L	1600 ± 200 nM
12	3,4-diCl-5-Me	$CH_2CH_2NH_3^+Cl^-$	CH_3		L	13 ± 4 nM
15a	4,5-diBr	iPr	H		/	100%
15b	4,5-diBr	iPr	H		/	87%
novobiocin						170 ± 20 nM

[a]Concentration of compound that inhibits the enzyme activity by 50%.

[b]Residual activity of the enzyme at 1 μM of the compound.

Table 2

Inhibitory activity of type II compounds **22a-d** and **23a-d** against DNA gyrase from *E. coli*.

Compd.	R¹	R²	R³	IC$_{50}$ (nM)[a] or RA (%)[b]
				E. coli gyrase
22a	4,5-diBr	Bn	Me	100%
22b	4,5-diBr	$CH_2CH_2N(Me)_2$	Me	88%
22c	4,5-diBr	iPr	Me	91%
22d	3,4-diCl-5-Me	iPr	Me	59%
23a	4,5-diBr	Bn	H	88 ± 0 nM
23b	4,5-diBr	$CH_2CH_2NH(Me)_2^+Cl^-$	H	82%
23c	4,5-diBr	iPr	H	400 ± 90 nM
23d	3,4-diCl-5-Me	iPr	H	91 ± 29 nM
novobiocin				170 ± 20 nM

[a]Concentration of compound that inhibits the enzyme activity by 50%.

[b]Residual activity of the enzyme at 1 μM of the compound.

Table 3

Inhibitory activity of selected compounds against DNA gyrase from *S. aureus* and topoisomerase IV from *E. coli* and *S. aureus*.

Compd.	IC$_{50}$ (μM)[a] or RA (%)[b]		
	S. aureus gyrase	*E. coli* topo IV	*S. aureus* topo IV
8c	5.9 ± 0.7 μM	78%	98%
8e	0.093 ± 0.065 μM	0.45 ± 0.12 μM	0.28 ± 0.20 μM
8f	1.6 ± 0.6 μM	7.4 ± 1.5 μM	1.3 ± 0.1 μM
8i	1.3 ± 0.0 μM	100%	99%
9b	0.39 ± 0.09 μM	89%	3.7 ± 0.3 μM
9d	89%	96%	98%
9e	0.11 ± 0.04 μM	0.53 ± 0.06 μM	3.2 ± 0.4 μM
10a	22 ± 10 μM	100%	92%
11a	0.75 ± 0.15 μM	11 ± 0 μM	12 ± 0 μM
12	1.0 ± 0.3 μM	0.57 ± 0.16 μM	0.96 ± 0.09 μM
23a	79%	42 ± 11 μM	39 ± 0 μM
23c	85%	100%	96%
23d	0.14 ± 0.02 μM	100%	12 ± 0 μM
novobiocin	0.041 ± 0.07 μM	11 ± 2 μM	27 ± 7 μM

[a]Concentration of compound that inhibits the enzyme activity by 50%.

[b]Residual activity of the enzyme at 1 μM of the compound.

Table 4

Minimum inhibitory concentrations (MICs) of compounds **7c, 8a, 8d, 8e, 8f, 9a, 9b, 10a, 11a, 11b** and **12** against *S. aureus* (ATCC 25923), *E. faecalis* (ATCC 29212) and *E. coli* (JW5503, a *tolC* deletion mutant).

Compd.	MIC (*μ*M)[a]		
	S. aureus (ATCC 25923)	*E. faecalis* (ATCC 29212)	*E. coli* (JW5503) *tolC*[b]
7c	n.d.[c]	n.d.	25 μM
8a	n.d.	>75 μM	n.d.
8d	n.d.	3.13 μM	n.d.
8e	n.d.	3.13 μM	50 μM
8f	n.d.	6.25 μM	n.d.
9a	50 μM	50 μM	25 μM
9b	50 μM	25 μM	25 μM
10a	n.d.	6.25 μM	n.d.
11a	3.13 μM	1.56 μM	n.d.
11b	n.d.	100 μM	n.d.
12	n.d.	n.d.	50 μM
ciprofloxacin	1.5 μM	3.0μM	0.015 μM

[a]MIC (minimum inhibitory concentration that inhibits the growth of bacteria by 90%) values against *E. faecalis, S. aureus* and *E. coli* JW5503 (*tolC*). Ciprofloxacin was used as a positive control.

[b]*E. coli* strain with mutated efflux pump.

[c]Not determined.

Table 5

Minimum inhibitory concentrations (MICs) of compound **11a** against a broad panel of Gram-positive and Gram-negative bacterial strains.

Compound 11a	MIC (μM)[a]
Gram-positive bacteria	
S. aureus (ATCC 29213)	4.17 μM
S. aureus (MRSA, ATCC 43300)	3.13 μM
E. faecium (VRE, ATCC 70022)	3.13 μM
Gram-negative bacteria	
E. coli (ATCC 25922)	No inhibition up to 50 μM
E. coli (MG1655)	No inhibition up to 50 μM
E. coli (BW 25113)	No inhibition up to 50 μM
E. coli (BW 25113) *tolC*[b]	No inhibition up to 50 μM
E. coli (BW 25113) *acrB*[b]	No inhibition up to 50 μM
E. coli (BW 25113) *dapF*[c]	No inhibition up to 50 μM
E. coli (BW 25113) *mrcB*[c]	No inhibition up to 50 μM
E. coli (BW 25113) *surA*[c]	No inhibition up to 50 μM
E. coli (ATCC 25922) + 50 μg/mL PAβN	4.6 μM
E. coli (MG1655) + 50 μg/mL PAβN	10.2 μM
E. coli (BW 25113) + 50 μg/mL PAβN	No inhibition up to 20 μM
E. coli (BW 25113) *dapF*[c] + 50 μg/mL PAβN	No inhibition up to 20 μM
E. coli (BW 25113) *mrcB*[c] + 50 μg/mL PAβN	No inhibition up to 20 μM
E. coli (BW 25113) *surA*[c] + 50 μg/mL PAβN	13.8 μM
E. coli (MG1655) R136-to-C mutant + 50 μg/mL PAβN	No inhibition up to 50 μM

[a] MIC (minimum inhibitory concentration that inhibits the growth of bacteria by 90%) measurements were performed according to the EUCAST guidelines in 3 independent measurements.

[b] *E. coli* strain with mutated efflux pump.

[c] *E. coli* strain with loss-of-function mutation in the gene involved in the cell wall formation.